Title: Dpp spreading is required for medial but not for lateral wing disc growth.

Authors: Harmansa S, Hamaratoglu F, Affolter M, Caussinus E

Journal: Nature

Year: 2015 Nov 19

Volume: 527

Issue: 7578

Pages: 317-22

DOI: 10.1038/nature15712

Dpp spreading is required for medial but not for lateral wing disc growth

Stefan Harmansa[1], Fisun Hamaratoglu[2], Markus Affolter[1,4], Emmanuel Caussinus[1,3]

[1]Growth & Development, Biozentrum, Klingelbergstrasse 50/70, University of Basel, 4056 Basel, Switzerland

[2]Center for Integrative Genomics, University of Lausanne, 1015 Lausanne, Switzerland

[3]Institute of Molecular Life Sciences (IMLS), University of Zurich, 8057 Zurich, Switzerland

[4]Correspondence: Markus.Affolter@unibas.ch

Summary

Drosophila Dpp has served as a paradigm to study morphogen-dependent growth control. However, the role of a Dpp gradient in tissue growth remains highly controversial. Two fundamentally different models have been proposed: The "temporal rule" model suggests that all cells of the wing imaginal disc divide upon a 50% increase in Dpp signalling, whereas the "growth equalization model" suggests that Dpp is only essential for proliferation control of the central cells. To discriminate between these two models, we generated and used morphotrap, a membrane-tethered anti-GFP nanobody, which allows immobilizing EGFP::Dpp on the cell surface, thereby completely abolishing Dpp gradient formation. We find that in the

absence of Dpp spreading, wing disc patterning is completely lost; however, lateral cells still divide at normal rates. These data are in line with the "growth equalization" model, but argue against a global "temporal rule" model in the wing imaginal disc.

Main text

Morphogens regulate patterning and growth of tissues and organs. They form long-range gradients from regions of high concentration (the source) to regions of low concentration (the adjacent target field)[1-5]. In *Drosophila*, the vertebrate BMP2/4 homolog Decapentaplegic (Dpp) was found to contribute to the formation of multiple tissues, and its role as a morphogen has been studied extensively in the wing imaginal disc. The wing imaginal disc, the larval precursor of the fly wing, grows from ≈40 to 50,000 cells during the four days of larval development, and is subdivided into an anterior and a posterior compartment[6,7]. Dpp is expressed in a stripe of anterior cells adjacent to the compartment boundary[8]. This stripe source of Dpp establishes long-range anterior and posterior extracellular gradients in the target field[9-11], the wing imaginal disc. The Dpp gradient is transduced by its receptors Thickveins (Tkv)[12] and Punt[13] and translated into an intracellular gradient of Phosphorylated Mothers against dpp (P-Mad)[14]. Together with Medea and Schnurri[15,16], P-Mad suppresses transcription of *brinker* (*brk*)[17-19], a repressor of Dpp target gene transcription and a repressor of growth[20]. This results in high P-Mad levels (high Dpp signalling) in the medial region of the wing disc and high Brk levels (low Dpp signalling) in the lateral region of the wing disc. The interplay of P-Mad and Brk coordinates the expression profiles of other Dpp targets, such as *spalt* (*sal*), *optomoter blind* (*omb*) and *daughters against Dpp* (*dad*)[21-23]. Sal and Omb define positions of the wing veins 2 and 5, respectively, and are also required for the survival of wing disc cells[24,25]. In addition to its role in patterning, Dpp is a key regulator of growth; overexpression of Dpp promotes wing disc overgrowth[26,27], while *dpp* mutant wing discs remain very small[28].

The requirement for Dpp spreading has never been explicitly tested by, for example, blocking Dpp dispersal by tethering it to the cell membrane, as it has been done for the Wingless (Wg) morphogen[29-31]. The available experimental evidence strongly supports an instructive and essential role for Dpp spreading in the control of patterning (reviewed in[14,32,33]). However, the role of Dpp spreading in growth control is highly controversial[5,32,34,35]. Two major models have been suggested to explain how the Dpp gradient controls uniform proliferation and growth of the wing disc. One model, the “temporal rule”, suggests that all cells of the wing imaginal disc compute the level of Dpp and divide upon a 50% increase in cellular

signalling levels. In contrast, the "growth equalization" model proposes that Dpp plays an indirect role in growth control primarily by equilibrating inherent, non-homogenous growth potentials across the A-P axis of the wing disc[32,35-38]. In this model, the proliferation of medial cells is sustained by the removal of the growth repressor Brk, while the proliferation rate of lateral cells (which have a higher growth potential) is limited by Brk to rates that can be sustained by medial cells, resulting in a uniform proliferation profile along the wing disc tissue. In the growth equalization model, the Dpp/Brk system is not a growth promoter but is rather a growth-modulatory system, ironing out inherent regional differences in proliferation rates[37]. To better study the role of Dpp spreading in wing disc patterning and growth, we designed and experimentally established a novel approach to manipulate morphogen gradients *in vivo*.

Nanobody-mediated morphogen trapping

In order to manipulate the Dpp gradient *in vivo*, we designed and implemented a synthetic morphogen trapping system consisting of a GFP-tagged morphogen (in our case, EGFP::Dpp) and of a generic extracellular GFP trap (VHH-GFP4::CD8::mCherry; referred to as morphotrap) (Fig.1a). Our EGFP::Dpp construct is based on a previously published fusion protein[9] and was implemented as a LexA inducible transgene[39] (see Methods). Of critical importance in our design, and in contrast to another GFP tagged Dpp protein[10], the EGFP tag was placed such that it cannot be cleaved away from the mature Dpp molecule[40] (Extended Data Fig.1a). Morphotrap (VHH-GFP4::CD8::mCherry) represents a fusion protein consisting of an extracellular, single-domain nanobody against GFP[41] (and cognate fluorescent tags, including EGFP), followed by the mouse CD8 transmembrane domain[42] and a cytoplasmic mCherry fluorescent tag. Morphotrap was implemented as a Gal4-inducible transgene[43] as well as a LexA-inducible transgene[39] (see Methods). The principle idea behind morphotrap is to immobilise the extracellular fraction of EGFP::Dpp in *Drosophila* tissues in a controlled spatial manner, either in the presence or the absence of wild type Dpp (Fig.1a).

We first tested whether our EGFP::Dpp fusion protein rescued wing-specific *dpp* mutant flies[9]. For this purpose, we used the *dpp-LG* LexA driver[39] in a $dpp^{d8/d12}$ background to express EGFP::Dpp in the regular disc expression pattern of *dpp*. Under these conditions, EGFP::Dpp formed a bilateral extracellular gradient in the wing disc (Extended Data Fig.1b-e') and restored proper Dpp signalling in the wing tissue such that the vein pattern was rescued to a large extend and adult flies developed (Extended Data Fig.1). These results show that our EGFP::Dpp fusion protein acts as a good surrogate for Dpp in the wing disc.

To test for localisation and expression of morphotrap, we expressed it in wing pouch cells using *nubbin-Gal4*. At the cellular level, morphotrap localized along the baso-lateral and the apical surfaces (below and above the junctional marker Discs large [Dlg], respectively) of the expressing cells (Fig. 1b). At the tissue level, when expressed at high levels in the posterior compartment using *hedgehog-Gal4*, morphotrap did not show any toxicity or interference with endogenous Dpp signalling (Extended Data Fig.2a-e). Therefore, morphotrap can be expressed at high levels and accumulates around the expressing wing disc cells without interfering with cell division and patterning.

Morphotrap can modify the Dpp gradient

We then tested whether exposing morphotrap on the cell surface locally modified the extracellular concentration of EGFP::Dpp. We generated random small clones of morphotrap in wild type wing discs expressing EGFP::Dpp in the expression domain of *dpp*. In order to set apart the induced clones from the cells expressing EGFP::Dpp, we used Gal4 and LexA drivers to induce morphotrap and EGFP::Dpp expression, respectively (Fig.1c', see Methods). In control discs, in which no clones were generated, EGFP::Dpp formed a bilateral extracellular concentration gradient visualized by sensitive extracellular immunostainings against EGFP (Fig.1d and Methods for quantification). The EGFP signal dropped below detection levels at a distance of app. ≈60 μm from the medial EGFP::Dpp source. In discs, in which small clones expressing morphotrap had been generated, we detected high levels of extracellular EGFP::Dpp

coating the surface of the clone cells, even when the clones were located in regions in which EGFP::Dpp could not be detected otherwise (Fig.1e). These results show that morphotrap is able to sequester high amounts of extracellular EGFP::Dpp, even in areas of low or non-detectable EGFP::Dpp.

To test whether the trapped EGFP::Dpp was active in signalling, we performed immuno-staining against P-Mad. We found that morphotrap clones located in the lateral region of the disc showed increased P-Mad levels, mainly along the edge facing the EGFP::Dpp source (Extended Data Fig.2 f-g). The results show that EGFP::Dpp disperses over the entire width of the disc, although its levels can normally not be detected above background levels using fluorescent microscopy in the lateral regions (see also Wartlick *et al.*[34]). We conclude that EGFP::Dpp can interact with its receptors when bound to the cell surface by morphotrap and that lateral cells can respond to Dpp.

In order to investigate whether morphotrap was able to interfere with the formation of the extracellular concentration gradient of EGFP::Dpp when expressed in the source cells, we expressed both EGFP::Dpp and morphotrap in wild type wing discs in the expression domain of *dpp*. Under these conditions, we did not detect any dispersal of EGFP::Dpp using antibody staining (Fig.1f), suggesting that EGFP::Dpp cannot leave the source region due to tethering to secreting cells. To test whether small amounts of EGFP::Dpp were still dispersing through the disc, we additionally generated random clones that expressed morphotrap. Clones expressing morphotrap in lateral cells did not accumulate any EGFP::Dpp on the cell surface, neither did clones in the vicinity of the EGFP::Dpp source (Fig.1g', see inserts). These results demonstrate that morphotrap fully traps EGFP::Dpp in source cells and completely abolishes the formation of the extracellular concentration gradient of EGFP::Dpp.

Dpp spreading is required for patterning

The function of *dpp* for patterning the wing disc has been elucidated by diverse means, including loss-of-function and gain-of-function genetic experiments[11,15,44]. However, it has not been tested directly whether

Dpp target gene expression depends on the Dpp long-range function or, in other words, how a loss of Dpp spreading would affect target gene expression. Morphotrap represents a novel and powerful tool to investigate the role of Dpp spreading in patterning and growth. We compared Dpp signalling responses in control $dpp^{d8/d12}$ wing discs rescued by EGFP::Dpp (EGFP::Dpp gradient is present) to Dpp signalling responses in $dpp^{d8/d12}$ wing discs expressing both EGFP::Dpp and morphotrap in the expression domain of *dpp* (EGFP::Dpp gradient is absent; see Methods; Fig.2a-d). We performed immunostainings against P-Mad, Brk, Sal, and Omb (the latter three representing proteins encoded by target genes of Dpp signalling). In control discs, P-Mad, Sal, and Omb formed three bilateral gradients of different widths, Sal being the narrowest and Omb being the widest (Fig.2c+g and Extended Data Fig.3a); Brk was only detected in the most lateral regions of the discs (Fig.2e+g). In contrast, when EGFP::Dpp and morphotrap were co-expressed, Dpp spreading and hence gradient formation was fully blocked throughout development (Extended Data Fig.4a-c). In these discs P-Mad, Sal and Omb gradients collapsed in the posterior compartment to a single row of cells abutting the anterior source of EGFP::Dpp (Fig.2d,h, Extended Data Fig.3b); high levels of Brk were detected in the medial posterior compartment up to the source of Dpp, except for a single row of cells abutting the compartment boundary (Fig.2f,h). Similar results were obtained regarding target gene expression in the anterior compartment upon trapping EGFP::Dpp in source cells (see Fig.2h and Extended Data Fig.3). In addition, we inhibited EGFP::Dpp dispersal in posterior cells only (Extended Data Fig.5); under these conditions P-Mad failed to form a long-range gradient and both Sal and Omb expression collapsed onto the narrow P-Mad domain. Hence, wing disc patterning in P-compartment was abolished (Extended Data Fig5a-f). Also wings of flies with blocked or reduced Dpp spreading lacked proper wing vein patterning (Extended Data Fig.3f and Extended Data Fig.8d). These results show that dispersal of Dpp is strictly required for the patterning function of Dpp.

Dpp spreading and growth control

Despite numerous studies addressing the role of Dpp in the control of growth of the wing imaginal disc, the conclusions drawn from different sets of experiments have remained highly controversial. In the "temporal rule" model[34,45], all disc cells compute the increase in Dpp levels and divide upon a gain of 50%. In sharp contrast, the "growth equalization" model[32] proposes that lateral cells proliferate independent of Dpp (Fig.3a). In line with this later model, Dpp signalling has been blocked in regions outside of the wing pouch in several studies, without much effect on cell proliferation[46,47]. However, it has not been possible to directly modulate the Dpp gradient at the protein level until now, making it difficult to interpret the requirement of Dpp long-range function in growth control.

In order to try to discriminate between these two growth control models, we aimed at using a different experimental approach, directly eliminating the Dpp gradient at the protein level using morphotrap. We have shown above that the elimination of the gradient leads to a complete absence of Dpp signalling, i.e. the target genes *sal* and *omb* are not expressed in the wing epithelium beyond the source cells and the immediate neighbours, and, more importantly, the Brk repressor is present at high levels in all cells beyond the Dpp source. Thus, the Dpp signalling pathway is not activated beyond the source cells and their immediate neighbours, neither by spurious levels of Dpp nor by a Dpp-independent manner (see also Conclusions). We compared the proliferation pattern of control $dpp^{d8/d12}$ wing discs rescued by EGFP::Dpp to the proliferation pattern of $dpp^{d8/d12}$ wing discs expressing both EGFP::Dpp and morphotrap in the expression domain of *dpp*, i.e. we compared the growth rates of wing disc cells in the presence and in the absence of EGFP::Dpp spreading. We visualized the proliferation pattern of such wing discs by staining for Phospho-Histone 3 (P-H3), a marker for mitotic cells. In wild type wing discs, cell proliferation was shown to be uniform in space in 3rd instar wing discs[7,48,49]. Our quantitative analyses showed that in discs rescued with EGFP::Dpp, the proliferation profile was uniform (Fig.3b+c). When the extracellular concentration gradient of Dpp was blocked via morphotrap expression in the source cells, uniform proliferation was still observed in the lateral parts of the disc, despite the lack of EGFP::Dpp in this area (Fig.3d+e). Furthermore, we did not detect a significant difference in the mitotic density (P-H3

spot density) between control discs and discs with blocked Dpp spreading at any time point during development (Fig.3f and Extended Data Fig.4g-i).

In addition, we have used the whole-tissue labelling tool Raeppli[50] to induce differently marked clones in control wing discs and in wing discs in which Dpp spreading was blocked by morphotrap (Fig.4). In order to directly compare the proliferation rate in the presence or the absence of Dpp spreading, we have induced colour-selection in clones at different time points of development and quantitatively evaluated the resulting clone size after defined time points (number of cells per clone). In control wing discs, clonal growth rates were homogeneous along the A/P axis (black dots in Fig.4c,g,k). When Dpp spreading was blocked, we observed that the majority of clones showed similar growth rates to control clones, and we did not find a significant difference in clonal proliferation between controls and discs with blocked Dpp spreading (Fig.4d,h,l). However, we also found low numbers of small clones (1-3 cells) in proximity to the A/P boundary (Extended Data Fig.6). These small clones were not found in control discs, in which Dpp spreading was normal. The presence of such small clones might hint towards the fact that a subpopulation of wing disc cells depend on Dpp signalling to divide and/or survive.

In summary, both, the P-H3 data and the Raeppli results suggest that the cells in the lateral Brk domain do not depend on Dpp signalling to proliferate (in contradiction with the "temporal rule" model), but rather that the proliferation rate is set by a Dpp-independent system (in line with the "growth equalization model).

Dpp spreading and size control

Using morphotrap in *dpp* mutant flies also allowed us to address how long-range spreading of Dpp affects wing disc size control. We quantified and compared the temporal growth profile of the posterior compartment of control $dpp^{d8/d12}$ wing discs rescued by EGFP::Dpp to the growth profile of $dpp^{d8/d12}$ wing discs co-expressing both, EGFP::Dpp and morphotrap in the expression domain of *dpp*. We performed immunostainings against Brk at different time points between 80 and 112 hours after egg laying (AEL). In

control discs, the posterior compartment doubled in width during the observed time window (Fig. 5a-d and Extended Data Fig. 7c); we delimited a medial low Brk (indicating high Dpp signalling) zone and a lateral high Brk (indicating low Dpp signalling) zone (see Methods), both zones increased in width at the same speed, keeping a constant relative proportion of 1:1 (Fig.5g), consistent with published data[51]. In discs, in which spreading of Dpp was abolished, the low Brk zone in the centre of the disc was reduced to a single medial row of cells in the posterior compartment (see above). During the observed time window, the lateral part of the posterior compartment showed similar widths and width increases as the lateral high Brk zone of the posterior compartment of control discs (Fig.5m). Similar growth profiles were seen in discs expressing EGFP::Dpp in the stripe and morphotrap in the posterior compartment (Extended Data Fig.5g). These results demonstrate that growth in the lateral region of the wing disc is independent of the extracellular Dpp gradient and does not depend on the dynamics of Dpp signalling.

However, and as can be seen in Fig.2f, there is a gap in Brk expression in the lateral most region of the posterior compartment, indicative of Dpp expression from another, laterally located source. Indeed, it has been shown that Dpp is expressed during third instar larval stage in a posterior, lateral position and exerts a patterning role on the wing imaginal disc. However, this late Dpp expression does not affect growth properties of wing disc cells[52]. Despite this, the additional Dpp source might complicate the interpretation of our growth analyses. To circumvent this problem, we also measured the growth properties in the anterior compartment in the absence of the EGFP::Dpp gradient (high uniform levels of Brk are indeed present in all cells outside the source). Indeed, we found that the lateral anterior region still grows despite the absence of the Dpp gradient and the lack of Dpp signalling (Fig.5l).

In contrast, the medial, Brk-negative region is lost when Dpp spreading is blocked, suggesting that Dpp dispersal is important for growth control of the medial region, in particular in the wing pouch area. We therefore quantified wing pouch size using the inner Wg-expression ring as a pouch marker. We measured the size of the pouch in *dpp* mutant discs rescued with EGFP::Dpp, and compared it to those of discs, in which either EGFP::Dpp dispersal was hindered in the posterior compartment only, or in which the release

of EGFP::Dpp from the anterior source was blocked entirely (Extended Data Fig.8). The size of the posterior pouch was much reduced (by approximately 40%) upon blocking Dpp spreading in the posterior compartment. The size of the posterior wing pouch was even more reduced (by more than 60%) upon trapping of EGFP::Dpp in the source. These results indicate that EGFP::Dpp spreading is essential for wing pouch growth. The analyses using the whole-tissue labelling technique Raeppli (Extended Data Fig.6) further showed that small clones were found in the posterior compartment close to the compartment boundary when morphotrap is expressed in source cells. Such clones were not found in control discs. Together, these data show that Dpp signalling plays an important role in proliferation control of medial wing pouch cells, as indicated by earlier studies[36,46,47], and further suggest that the range of Dpp spreading might be crucially linked to the size of the wing pouch region along the AP axis.

Conclusions

Here, we have used morphotrap, a novel approach to manipulate the extracellular Dpp gradient in the wing imaginal disc. Expressing morphotrap in lateral wing disc cells captures EGFP::Dpp in regions of the disc, in which EGFP::Dpp cannot be detected above background levels. This finding demonstrates that Dpp does disperse over the entire wing imaginal disc, and that Dpp could control cell behaviour even in lateral regions. In agreement with this, recent data indicate that Dpp signalling is important for patterning the lateral region[53]. However, we find that while Dpp spreading is strictly required for wing disc patterning, it is not essential for cell proliferation in the lateral region of the wing disc. These results are in line with the "growth equalization" model but are in disagreement with a disc-wide "temporal rule" model, suggesting that lateral cells do not compute Dpp signalling levels to trigger cell division. It has been argued before that Dpp-independent Dpp signalling (in addition to Dpp-dependent Dpp signalling) might control cell proliferation according to the "temporal rule" model[54]. This interpretation was based on the observation that in genetic experiments, in which Dpp signalling was eliminated by the concomitant genetic removal of *brk* and *tkv* (or *brk* and *mad*), certain Dpp targets were still active due to the absence of

the potent Brk repressor[35,45]. However, in our experiments using morphotrap, Dpp signalling was eliminated via the removal of the Dpp gradient and lead to the absence of Dpp target gene expression and to the presence of high levels of Brk in the entire lateral wing disc. Therefore, in our experimental setting, Dpp signalling was turned off in the lateral cells, yet these cells divided at a normal rate, as quantitatively shown by our experiments using Raeppli. Since cell division should be abolished (or altered) in the absence of Dpp signalling, according to the "temporal rule", our experiments reject a general, disc-wide "temporal rule" model for wing disc growth control.

However, our data is entirely consistent with the proposal of the "growth equalization" model, suggesting that Dpp spreading results in medial removal of Brk and that this repression of *brk* represents an essential step in the formation of the wing pouch tissue[36]. Our results support the suggestion made by the "growth equalization" model, that the wing disc tissue consists of two regions with different requirements for Dpp signalling, namely a medial regions that depends on Dpp signalling to grow and a lateral region that grows independent of Dpp.

While the "growth equalization" model does not explain final organ size, our results suggest that the range of Dpp spreading is linked to the size of the wing pouch. In a number of elegant studies, the range of Wg signalling was suggested to control pouch growth via a feed-forward recruitment mechanism[31,55], presumably together with Dpp[55]. A better understanding of the role of Dpp signalling in the formation of the wing pouch will require manipulation of either the Dpp or the Wg signalling pathways (or both) using different means and to study in a comprehensive manner the downstream target genes of the two pathways and their mutual interactions as well as the proliferation patterns upon these alterations. The addition of the morphotrap and the Raeppli techniques to such analyses will help in gaining better insight into how morphogens control organ growth.

Methods

Fly strains

The following fly lines were used: y^1w^{1118} (wild type), *dpp-LG86Fb* and *LOP::mCherry-CAAX* (K. Basler), *tub>CD2,Stop>Gal4* (F. Pignioni). *P{Cre}1b* was obtained from Bloomington. *hh-Gal4*, *dpp-Gal4*, *nub-Gal4,* dpp^{d8} and dpp^{d12} are described on Flybase (www.flybase.org).

Genotypes by figure:

Figure 1: **b**, w; nub-Gal4 / UAS-morphotrap **d**, w; LOP-EGFP::Dpp / +; dpp-LG / + **e**, yw, hsFlp; tub>CD2,Stop>Gal4, LOP-EGFP::Dpp / UAS-morphotrap ; dpp-LG / + **f**, w; LOP-EGFP::Dpp / LOP-morphotrap ; dpp-LG / + **g**, w hsFlp ; LOP-EGFP::Dpp, tub>CD2,Stop>Gal4 / LOP/UAS-morphotrap ; dpp-LG / +

Figure 2: **a,c,e**, w; LOP-EGFP::Dpp, dpp^{d12} / dpp^{d8} ; dpp-LG / + **b,d,f**, w; LOP-EGFP::Dpp, dpp^{d12} / LOP-morphotrap, dpp^{d8} ; dpp-LG / +

Figure 3: **b-c**, w; LOP-EGFP::Dpp, dpp^{d12} / dpp^{d8} ; dpp-LG / + **d-e**, w; LOP-EGFP::Dpp, dpp^{d12} / LOP-morphotrap, dpp^{d8} ; dpp-LG / +

Figure 4: **a,e,i**, yw, hsFlp; LOP-EGFP::Dpp, dpp^{d12} / dpp^{d8} ; dpp-LG, hh-Gal4 / 2xLOP/UAS::Raeppli **b,f,j**, yw, hsFlp; LOP-EGFP::Dpp, dpp^{d12} / LOP-morphotrap, dpp^{d8} ; dpp-LG, hh-Gal4 / 2xLOP/UAS::Raeppli

Figure 5: **a-d**, w; LOP-EGFP::Dpp, dpp^{d12} / dpp^{d8} ; dpp-LG / + **h-k**, w; LOP-EGFP::Dpp, dpp^{d12} / LOP-morphotrap, dpp^{d8} ; dpp-LG / +

Molecular Cloning

pUASTLOTattB_EGFP::Dpp. GFP was replaced by EGFP in the Dpp-GFP plasmid[9] (obtained from S.Cohen). Then, EGFP::Dpp was inserted in the multiple cloning site of pUASTLOTattB vector[50] by standard cloning procedures.

pUASTLOTattB_VHH-GFP4::CD8::mCherry. We inserted the VHH-GFP4 fragment after the signal peptide sequence of the mouse CD8 domain in the pUAS::CD8::GFP plasmid[42]. We replaced the GFP by a mCherry (Clonetech) and finally cloned the VHH-GFP4::CD8::mCherry fragment into the pUASTLOTattB vector[50].

Transgenes were inserted by phiC31 integrase mediated recombination into the 35B region on the 2nd chromosome. Resulting fly lines are responsive to LexA and Gal4 transcriptional activators. By crossing these flies to *Cre*^{y} expressing flies, either the UAS or the LOP site is being excised in a mutually exclusive manner. Excision was screened for by PCR as described in Kanca *et. al.*[50]

Creation of Wing Disc Datasets

Flies were kept in standard fly vials (containing polenta and yeast) in a 26°C incubator. Larvae were staged as described in Hamaratoglu *et. al.*[51]. In our datasets, we only included male larvae, which were positively selected for the presence of the genital disc. Larvae of different genotypes were dissected and processed together using identical solutions.

Immunostainings and Image Acquisition

Staged larvae were dissected and transferred directly to cold fixative (4% PFA in PBS) and fixed for 20 min at room temperature (RT) or 40min at 4°C (for P-Mad and Brk stainings) rotating. After fixation, discs were extensively washed with PBT (PBS + 0.3% TritonX) and blocked in PBTN (PBT + 2% Normal Donkey Serum, Jackson Immuno Research Laboratories) for 30 min at RT, followed by incubation with primary antibody overnight at 4°C. The next day discs were washed in PBT 6 times 20 min and incubated in secondary antibody for 1.5h at RT on a rotor. Following another round of washes with PBT samples were mounted in Vectashield (H-1000, Vector Laboratories). All discs of one data-set were mounted on

the same slide using larval brains as spacers. For all quantitative data-sets we made sure that imaging conditions allowed acquisition of data in the linear range (Extended Data Fig.6). For high resolution imaging along the z-axis (Fig.1b), discs were mounted with double sided tape as spacers to avoid squeezing of the discs. The extracellular GFP staining was done as described in Strigini *et. al.*[56]. Images were acquired on a Leica SP5 confocal microscope (Section thickness 1 µm for data-sets, 0.13 µm for optical cross section in Fig.1b.

Antibodies

rb-α-P-Mad (1:1500, Ed Laufer); rb-α-Phospho-Smad1/5 (1:200, Cell Signaling, 9516S, used in Extended Data Fig.4d-f); gp-α-Brk (1:1000, Gines Morata); rb-α-Sal (1:40, Reinhard Schuh); rat-αSal (1:700, Rosa Barrio); rb-α–Omb (1:1200, Gert O. Plugfelder); m-α-Wg (a.k.a. 4D4-s, 1:120, DSHB, University of Iowa); m-α-Ptc (a.k.a. Apa1-s, 1:40, DSHB, University of Iowa); rb-α-GFP (1:200 for extracellular staining, Abcam ab6556). All secondary antibodies from the AlexaFluor series were used at 1:750 dilutions except for Alexa405-α-rb and Alexa680-α-m, which were used at 1:500 dilutions; CF405S-α-gp was used 1:1000 (Sigma-Aldrich).

Image Processing

Images were processed using ImageJ (NIH) software. Concentration profiles in Figure 1, Extended Data Figure 3 and Extended Data Figure 4f'' were created using the Plot Profile function in ImageJ. Optical cross section in Figure 1b was created using the section function in Imaris (Bitplain) software. We made use of the Wg/Ptc co-staining[51] which outlines the wing pouch (Wg), the D/V boundary (Wg) and the A/P boundary (Ptc, also see Extended Data Fig.2). Quantification of wing pouch size and extraction of average gradient profiles (Fig.2g-h, Fig.3f, Extended Data Fig.1f, Extended Data Fig.2d-e, Extended Data Fig.4c,f,I, Extended Data Fig.5e, Extended Data Fig.8g) were done using the WingJ software[57] (http://lis.epfl.ch/wingj). For measuring gradient profiles in WingJ we used average projections of 10 consecutive slices spanning the disc proper epithelium only. Gradient profiles were extracted using WingJ software either only in the pouch (Extended Data Fig.2) or up to the edge of the wing disc (Fig.2,

Extended Data Fig.4), which allowed a better representation of lateral Brk profiles. Profiles were measured with a Sigma of 4px and either 15% ventral offset (for Extended Data Fig.2e) or 30% dorsal offset (for all other profiles) parallel to the D/V border (marked by the Wg staining). Statistical analysis on wing pouch size and plotting of average concentration profiles was done applying the Matlab toolbox included in WingJ using the Matlab (Matworks) software.

Generation of mitotic density maps

Wing discs were staged and stained for Wg/Ptc and P-H3, a marker labelling mitotic cells. P-H3 positive nuclei were detected using the Imaris software (Bitplane) spot detection tool; peripodial nuclei were excluded from the following computation. Each disc was marked at 15 landmarks (see Extended Data Fig.5a). 16 discs of one time point were fitted to a reference disc using these landmarks by an affine transformation (least square, Fiji - Landmark correspondence plug-in). All data points of these 16 discs were included in a scatter plot using the Scatplot script (Alejandro Sanchez-Barba, 2005, http://www.mathworks.com/matlabcentral/fileexchange/8577-scatplot) in Matlab. The Scatplot visualizes data point density by a colour map, with high-density regions appearing in red and low-density regions in blue.

Induction and computation of Raeppli clones

In our experiments we used two copies of nuclear Raeppli, resulting in 10 different colour combinations after induction (see Kanca *et.al.*). The larvae were staged as described above and dissected at 96-100h AEL. Raeppli was induced by heat shock (38°C for 15 min.) at three different developmental time points: 55-59h AEL (~43h before dissection), 68-72h AEL (~30h before dissection) or 78-82h AEL (~20h before dissection). Discs were fixed in 4% PFA in PBS for 20 min at RT, washed in PBT extensively and mounted in Vectashield (H-1000, Vector Laboratories). Images were acquired on a Leica SP5 confocal microscope using the settings suggested in Kanca *et.al.*[50]. Number of cells per clone was counted using the "multi-point tool" in ImageJ software (NIH).

Measuring growth of the medial and lateral domain of the wing disc

In order to compare the growth dynamics of the medial (high Dpp signalling) and the lateral domain (low Dpp signalling), we define the position of half-maximum Brk levels as the boundary between these two domains. The position of half-maximum Brk levels was accessed by extracting Brk intensity profiles along a straight line with 30% dorsal offset parallel to the D/V boundary (Extended Data Fig.5d-1) in each disc individually. Subsequently single Brk profiles – separately for the anterior and the posterior compartment - were fit to a Hill-function (see Extended Data Fig.5d-3.) using the fitting-toolbox in Matlab. For fitting we excluded the lateral most signal, which is noisy due to folds and signal form the peripodial membrane. The Hill function to which we fit the Brk profiles returns four parameters: the amplitude A, a measure for how sharp the profile drops n, a constant offset C, and the position of half-maximum Brk levels k (k_A and k_P for the anterior and the posterior compartment, respectively). To access the width of the lateral domain, we measured the width of the full compartment L_A and L_P for the anterior and the posterior compartment, respectively. Since k_A equals the width of the anterior medial domain, L_A-k_A equals the width of the anterior lateral region, and accordingly L_P-k_P the width of the posterior lateral domain. Medial domain width in case of the posterior compartment in EGFP::Dpp morphotrap co-expressing wing discs was not fit to a Hill-function, since in this condition only one cell row experiences Dpp signalling during the observed time window (equalling a width of 3.5µm on average).

References

1 Ashe, H. L. & Briscoe, J. The interpretation of morphogen gradients. *Development* **133**, 385-394, doi:10.1242/dev.02238 (2006).

2 Baena-Lopez, L. A., Nojima, H. & Vincent, J. P. Integration of morphogen signalling within the growth regulatory network. *Current opinion in cell biology* **24**, 166-172, doi:10.1016/j.ceb.2011.12.010 (2012).

3 Rogers, K. W. & Schier, A. F. Morphogen gradients: from generation to interpretation. *Annual review of cell and developmental biology* **27**, 377-407, doi:10.1146/annurev-cellbio-092910-154148 (2011).

4 Schwank, G. & Basler, K. Regulation of organ growth by morphogen gradients. *Cold Spring Harbor perspectives in biology* **2**, a001669, doi:10.1101/cshperspect.a001669 (2010).

5 Wartlick, O., Mumcu, P., Julicher, F. & Gonzalez-Gaitan, M. Understanding morphogenetic growth control -- lessons from flies. *Nature reviews. Molecular cell biology* **12**, 594-604, doi:10.1038/nrm3169 (2011).

6 Martin, F. A., Herrera, S. C. & Morata, G. Cell competition, growth and size control in the Drosophila wing imaginal disc. *Development* **136**, 3747-3756, doi:10.1242/dev.038406 (2009).

7 Garcia-Bellido, A. & Merriam, J. R. Parameters of the wing imaginal disc development of Drosophila melanogaster. *Developmental biology* **24**, 61-87 (1971).

8 Masucci, J. D., Miltenberger, R. J. & Hoffmann, F. M. Pattern-specific expression of the Drosophila decapentaplegic gene in imaginal disks is regulated by 3' cis-regulatory elements. *Genes & development* **4**, 2011-2023 (1990).

9 Teleman, A. A. & Cohen, S. M. Dpp gradient formation in the Drosophila wing imaginal disc. *Cell* **103**, 971-980 (2000).

10 Entchev, E. V., Schwabedissen, A. & Gonzalez-Gaitan, M. Gradient formation of the TGF-beta homolog Dpp. *Cell* **103**, 981-991 (2000).

11 Nellen, D., Burke, R., Struhl, G. & Basler, K. Direct and long-range action of a DPP morphogen gradient. *Cell* **85**, 357-368 (1996).

12 Nellen, D., Affolter, M. & Basler, K. Receptor serine/threonine kinases implicated in the control of Drosophila body pattern by decapentaplegic. *Cell* **78**, 225-237 (1994).

13 Ruberte, E., Marty, T., Nellen, D., Affolter, M. & Basler, K. An absolute requirement for both the type II and type I receptors, punt and thick veins, for dpp signaling in vivo. *Cell* **80**, 889-897 (1995).

14 Affolter, M. & Basler, K. The Decapentaplegic morphogen gradient: from pattern formation to growth regulation. *Nature reviews. Genetics* **8**, 663-674, doi:10.1038/nrg2166 (2007).

15 Muller, B., Hartmann, B., Pyrowolakis, G., Affolter, M. & Basler, K. Conversion of an extracellular Dpp/BMP morphogen gradient into an inverse transcriptional gradient. *Cell* **113**, 221-233 (2003).

16 Pyrowolakis, G., Hartmann, B., Muller, B., Basler, K. & Affolter, M. A simple molecular complex mediates widespread BMP-induced repression during Drosophila development. *Developmental cell* **7**, 229-240, doi:10.1016/j.devcel.2004.07.008 (2004).

17 Jazwinska, A., Kirov, N., Wieschaus, E., Roth, S. & Rushlow, C. The Drosophila gene brinker reveals a novel mechanism of Dpp target gene regulation. *Cell* **96**, 563-573 (1999).

18 Minami, M., Kinoshita, N., Kamoshida, Y., Tanimoto, H. & Tabata, T. brinker is a target of Dpp in Drosophila that negatively regulates Dpp-dependent genes. *Nature* **398**, 242-246, doi:10.1038/18451 (1999).

19 Campbell, G. & Tomlinson, A. Transducing the Dpp morphogen gradient in the wing of Drosophila: regulation of Dpp targets by brinker. *Cell* **96**, 553-562 (1999).

20 Doumpas, N. *et al.* Brk regulates wing disc growth in part via repression of Myc expression. *EMBO reports* **14**, 261-268, doi:10.1038/embor.2013.1 (2013).

21 Barrio, R. & de Celis, J. F. Regulation of spalt expression in the Drosophila wing blade in response to the Decapentaplegic signaling pathway. *Proceedings of the National Academy of Sciences of the United States of America* **101**, 6021-6026, doi:10.1073/pnas.0401590101 (2004).

22 Weiss, A. *et al.* A conserved activation element in BMP signaling during Drosophila development. *Nature structural & molecular biology* **17**, 69-76, doi:10.1038/nsmb.1715 (2010).

23 Sivasankaran, R., Vigano, M. A., Muller, B., Affolter, M. & Basler, K. Direct transcriptional control of the Dpp target omb by the DNA binding protein Brinker. *The EMBO journal* **19**, 6162-6172, doi:10.1093/emboj/19.22.6162 (2000).

24 Cook, O., Biehs, B. & Bier, E. brinker and optomotor-blind act coordinately to initiate development of the L5 wing vein primordium in Drosophila. *Development* **131**, 2113-2124, doi:10.1242/dev.01100 (2004).

25 Organista, M. F. & De Celis, J. F. The Spalt transcription factors regulate cell proliferation, survival and epithelial integrity downstream of the Decapentaplegic signalling pathway. *Biology open* **2**, 37-48, doi:10.1242/bio.20123038 (2013).

26 Capdevila, J. & Guerrero, I. Targeted expression of the signaling molecule decapentaplegic induces pattern duplications and growth alterations in Drosophila wings. *The EMBO journal* **13**, 4459-4468 (1994).

27 Zecca, M., Basler, K. & Struhl, G. Sequential organizing activities of engrailed, hedgehog and decapentaplegic in the Drosophila wing. *Development* **121**, 2265-2278 (1995).

28 Spencer, F. A., Hoffmann, F. M. & Gelbart, W. M. Decapentaplegic: a gene complex affecting morphogenesis in Drosophila melanogaster. *Cell* **28**, 451-461 (1982).

29 Zecca, M. & Struhl, G. Recruitment of cells into the Drosophila wing primordium by a feed-forward circuit of vestigial autoregulation. *Development* **134**, 3001-3010, doi:10.1242/dev.006411 (2007).

30 Alexandre, C., Baena-Lopez, A. & Vincent, J. P. Patterning and growth control by membrane-tethered Wingless. *Nature* **505**, 180-185, doi:10.1038/nature12879 (2014).

31 Zecca, M. & Struhl, G. A feed-forward circuit linking wingless, fat-dachsous signaling, and the warts-hippo pathway to Drosophila wing growth. *PLoS biology* **8**, e1000386, doi:10.1371/journal.pbio.1000386 (2010).

32 Restrepo, S., Zartman, J. J. & Basler, K. Coordination of patterning and growth by the morphogen DPP. *Current biology : CB* **24**, R245-255, doi:10.1016/j.cub.2014.01.055 (2014).

33 Hamaratoglu, F., Affolter, M. & Pyrowolakis, G. Dpp/BMP signaling in flies: from molecules to biology. *Seminars in cell & developmental biology* **32**, 128-136, doi:10.1016/j.semcdb.2014.04.036 (2014).

34 Wartlick, O. *et al.* Dynamics of Dpp signaling and proliferation control. *Science* **331**, 1154-1159, doi:10.1126/science.1200037 (2011).

35 Schwank, G., Yang, S. F., Restrepo, S. & Basler, K. Comment on "Dynamics of dpp signaling and proliferation control". *Science* **335**, 401; author reply 401, doi:10.1126/science.1210997 (2012).

36 Martin, F. A., Perez-Garijo, A., Moreno, E. & Morata, G. The brinker gradient controls wing growth in Drosophila. *Development* **131**, 4921-4930, doi:10.1242/dev.01385 (2004).

37 Schwank, G., Restrepo, S. & Basler, K. Growth regulation by Dpp: an essential role for Brinker and a non-essential role for graded signaling levels. *Development* **135**, 4003-4013, doi:10.1242/dev.025635 (2008).

38 Schwank, G. *et al.* Antagonistic growth regulation by Dpp and Fat drives uniform cell proliferation. *Developmental cell* **20**, 123-130, doi:10.1016/j.devcel.2010.11.007 (2011).

39 Yagi, R., Mayer, F. & Basler, K. Refined LexA transactivators and their use in combination with the Drosophila Gal4 system. *Proceedings of the National Academy of Sciences of the United States of America* **107**, 16166-16171, doi:10.1073/pnas.1005957107 (2010).

40 Kunnapuu, J., Bjorkgren, I. & Shimmi, O. The Drosophila DPP signal is produced by cleavage of its proprotein at evolutionary diversified furin-recognition sites. *Proceedings of the National Academy of Sciences of the United States of America* **106**, 8501-8506, doi:10.1073/pnas.0809885106 (2009).

41 Saerens, D. *et al.* Identification of a universal VHH framework to graft non-canonical antigen-binding loops of camel single-domain antibodies. *Journal of molecular biology* **352**, 597-607, doi:10.1016/j.jmb.2005.07.038 (2005).

42 Lee, T. & Luo, L. Mosaic analysis with a repressible cell marker for studies of gene function in neuronal morphogenesis. *Neuron* **22**, 451-461 (1999).

43 Brand, A. H. & Perrimon, N. Targeted gene expression as a means of altering cell fates and generating dominant phenotypes. *Development* **118**, 401-415 (1993).

44 Lecuit, T. *et al.* Two distinct mechanisms for long-range patterning by Decapentaplegic in the Drosophila wing. *Nature* **381**, 387-393, doi:10.1038/381387a0 (1996).

45 Wartlick, O., Mumcu, P., Jülicher, F. & Gonzalez-Gaitan, M. Response to Comment on "Dynamics of Dpp Signaling and Proliferation Control". *Science* **335**, 401, doi:DOI: 10.1126/science.1211373 (2012).

46 Martin-Castellanos, C. & Edgar, B. A. A characterization of the effects of Dpp signaling on cell growth and proliferation in the Drosophila wing. *Development* **129**, 1003-1013 (2002).

47 Burke, R. & Basler, K. Dpp receptors are autonomously required for cell proliferation in the entire developing Drosophila wing. *Development* **122**, 2261-2269 (1996).

48 Milan, M., Campuzano, S. & Garcia-Bellido, A. Cell cycling and patterned cell proliferation in the wing primordium of Drosophila. *Proceedings of the National Academy of Sciences of the United States of America* **93**, 640-645 (1996).

49 Mao, Y. *et al.* Differential proliferation rates generate patterns of mechanical tension that orient tissue growth. *The EMBO journal* **32**, 2790-2803, doi:10.1038/emboj.2013.197 (2013).

50 Kanca, O., Caussinus, E., Denes, A. S., Percival-Smith, A. & Affolter, M. Raeppli: a whole-tissue labeling tool for live imaging of Drosophila development. *Development* **141**, 472-480, doi:10.1242/dev.102913 (2014).

51 Hamaratoglu, F., de Lachapelle, A. M., Pyrowolakis, G., Bergmann, S. & Affolter, M. Dpp signaling activity requires Pentagone to scale with tissue size in the growing Drosophila wing imaginal disc. *PLoS biology* **9**, e1001182, doi:10.1371/journal.pbio.1001182 (2011).

52 Foronda, D., Perez-Garijo, A. & Martin, F. A. Dpp of posterior origin patterns the proximal region of the wing. *Mechanisms of development* **126**, 99-106, doi:10.1016/j.mod.2008.12.002 (2009).

53 Ziv, O. *et al.* Inverse regulation of target genes at the brink of the BMP morphogen activity gradient. *Journal of cell science* **125**, 5811-5818, doi:10.1242/jcs.110569 (2012).

54 Wartlick, O., Julicher, F. & Gonzalez-Gaitan, M. Growth control by a moving morphogen gradient during Drosophila eye development. *Development* **141**, 1884-1893, doi:10.1242/dev.105650 (2014).

55 Zecca, M. & Struhl, G. Control of Drosophila wing growth by the vestigial quadrant enhancer. *Development* **134**, 3011-3020, doi:10.1242/dev.006445 (2007).

56 Strigini, M. & Cohen, S. M. Wingless gradient formation in the Drosophila wing. *Current biology : CB* **10**, 293-300 (2000).

57 Schaffter, T. *From genes to organisms: Bioinformatics System Models and Software*, École polytechnique fédérale de Lausanne, (2014).

Supplementary information is linked to the online version of the paper at www.nature.com/nature

Acknowledgements We thank S. Matsuda, I. Alborelli and H. Belting for discussions; T. Schaffter for help and support with WingJ; the Biozentrum Imaging Core Facility for maintenance of microscopes and support. We are grateful to G. Struhl, K. Basler and G. Pyrowolakis for their input and discussion on the project. We thank K. Basler, S. Cohen, G. Morata, R. Bario and E. Laufer for flies and reagents. SH was supported by the "Fellowships for Excellence" International PhD Program in Molecular Life Sciences of the Biozentrum, University of Basel Switzerland. E.C. was funded by the SystemsX.ch initiative within the framework of the WingX and the MorphogenetiX projects. F.H. is supported by a SNSF Professorship grant (PP00P3_150682). The work in the lab was supported by grants from Cantons Basel-Stadt and Basel-Land and from the Swiss National Science Foundation (M.A.).

Author Contributions S.H., E.C., F.H. and M.A. conceived and designed the study. S.H. performed the experiments. S.H. analyzed the data. S.H., E.C. and M.A. wrote the paper.

Author Information Reprints and permissions information is available at www.nature.com/reprints. The authors declare no competing financial interests. Correspondence and requests for materials should be addressed to M.A. (Markus. Affolter@unibas.ch)

Main figures

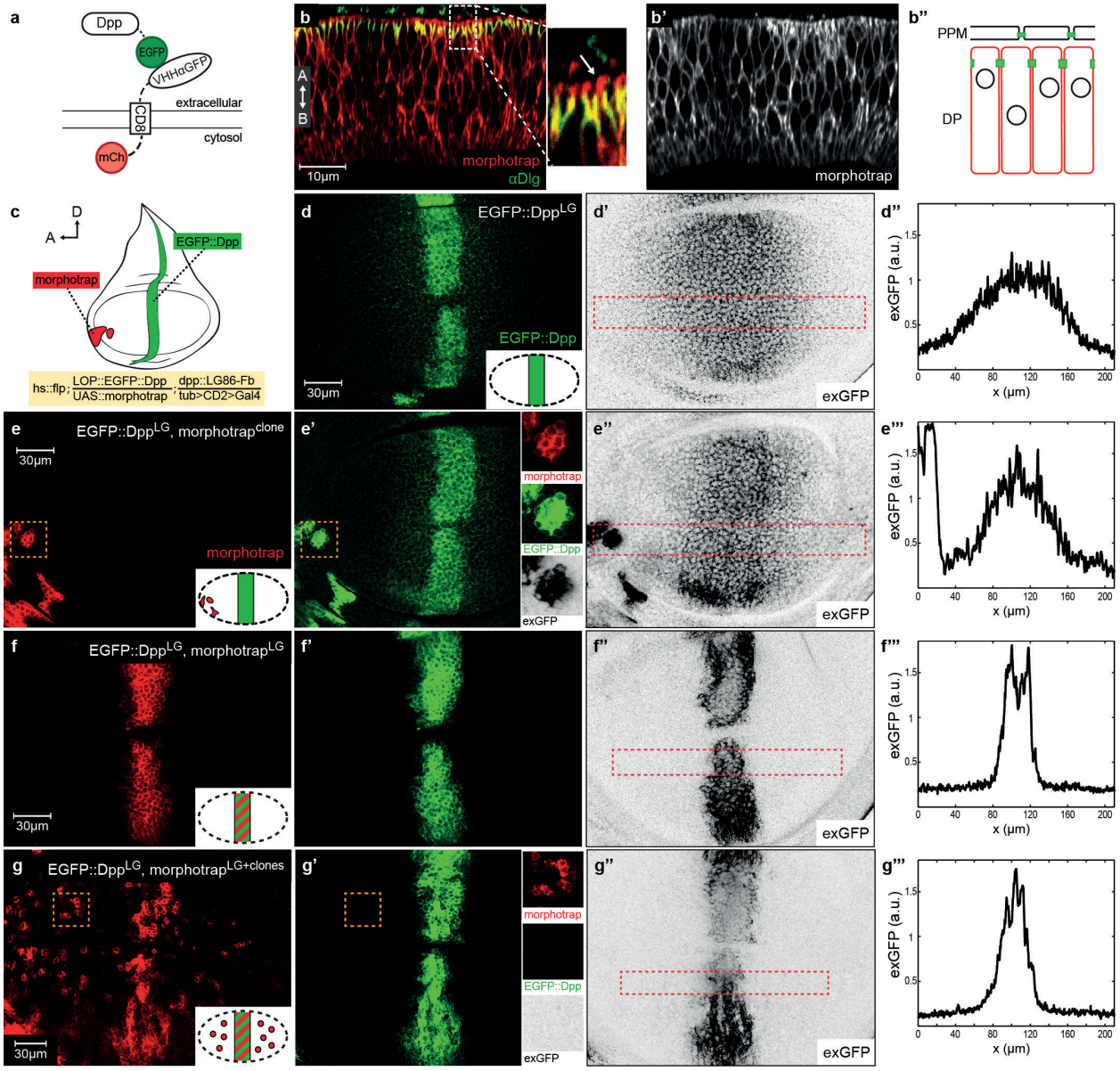

Figure 1 – Morphotrap can block EGFP::Dpp spreading

a, The morphotrap system. **b**, Optical-cross section (**b-b'**) and schematics (**b''**) of a morphotrap expressing wing disc. Morphotrap is localized all along the cell membrane (in red), both apical (arrow) and basal to Dlg (in green). **c**, Schematic representation of EGFP::Dpp (LexA/LOP) and morphotrap clones (Gal4/UAS). **d**, A wild type wing disc expressing EGFP::Dpp in the Dpp stripe (dpp::LG), visualized by EGFP fluorescence (**d**) or by extracellular GFP staining (exGFP) (**d'**).Fluorescence intensity profile of the region marked by a red rectangle (d''). **e**, Lateral morphotrap clones trap extracellular

EGFP::Dpp. **f**, Gradient formation is blocked by co-expression of EGFP::Dpp and morphotrap in the Dpp stripe (both expressed by dpp::LG). **g**, Co-expression of EGFP::Dpp and Morphotrap in the stripe (dpp::LG) fully block Dpp spreading since morphotrap clones do not show EGFP signal. (see inserts in **g'**).

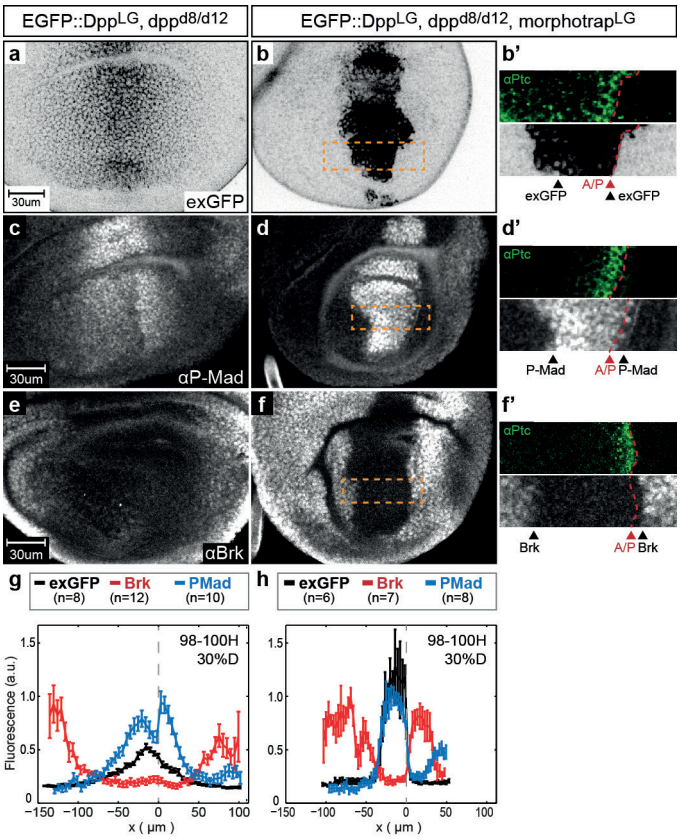

Figure 2 - Blocking Dpp spreading results in a sharp P-Mad/Brk transition

a, Representative *dpp*$^{d8/d12}$ mutant wing disc rescued with EGFP::Dpp (rescue) and stained for exGFP (gray). **b**, exGFP signal in a disc co-expressing EGFP::Dpp and morphotrap (*dpp-LG*, co-expression) in a *dpp*$^{d8/d12}$ mutant. **b'**, Magnification of the region marked by the rectangle in (**b**), showing that all signal is from anterior cells where Dpp is expressed. A/P boundary is determined by Ptc staining (green) and marked by dotted line. Approximate domain size is marked by arrowheads. **c-d**, P-Mad staining in rescue (**c**) and co-expression (**d**) wing discs. **e-f**, Brk staining in rescue (**e**) and co-expression (**f**) wing discs. **g-f**, Average fluorescence intensity profiles measured to the edge of the wing disc of rescued (**g**) and co-expression (**h**) wing discs. (Error bars show standard deviation)

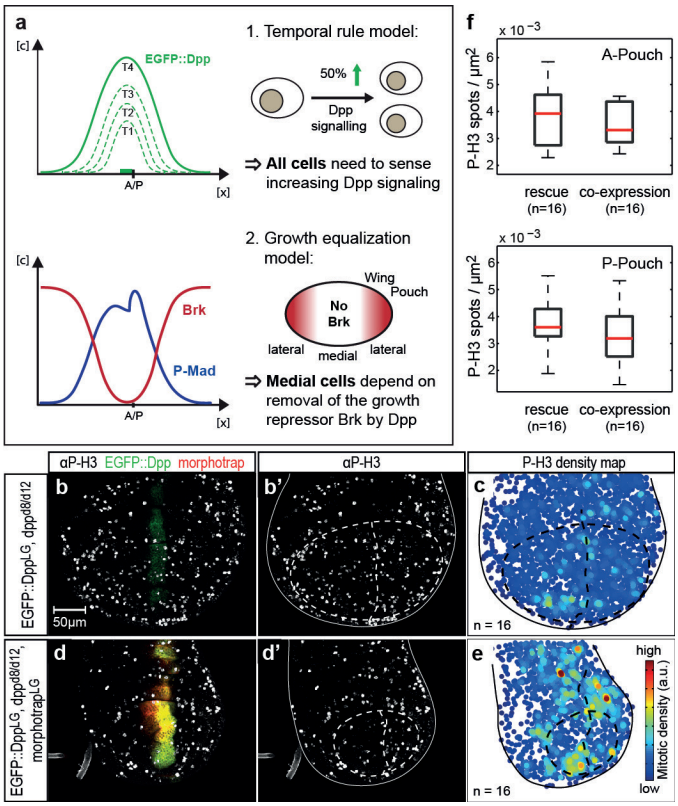

Figure 3 – The uniform proliferation pattern is independent of Dpp spreading

a, top row: the "Temporal rule" model of growth control. Bottom row: the "Growth Equalization" model. **b**, P-H3 staining in a representative *dpp*$^{d8/d12}$ mutant wing disc rescued with EGFP::Dpp. The A/P boundary and the pouch outlines are marked by dotted lines (in **b'**). **c, e**, Computed P-H3 spots density (of n=16 discs) in rescue (**c**) and co-expression (**e**) wing discs (see Methods). **d**, P-H3 signal in a *dpp*$^{d8/d12}$ mutant wing disc co-expressing EGFP::Dpp and morphotrap. **f**, Mitotic density in the anterior and posterior pouch (whiskers correspond to minimum and maximum data points). No significant differences were detected (2-sided *t*-test with unequal variance). All images are shown at the same magnification; scale bar in (**b**) is 50µm.

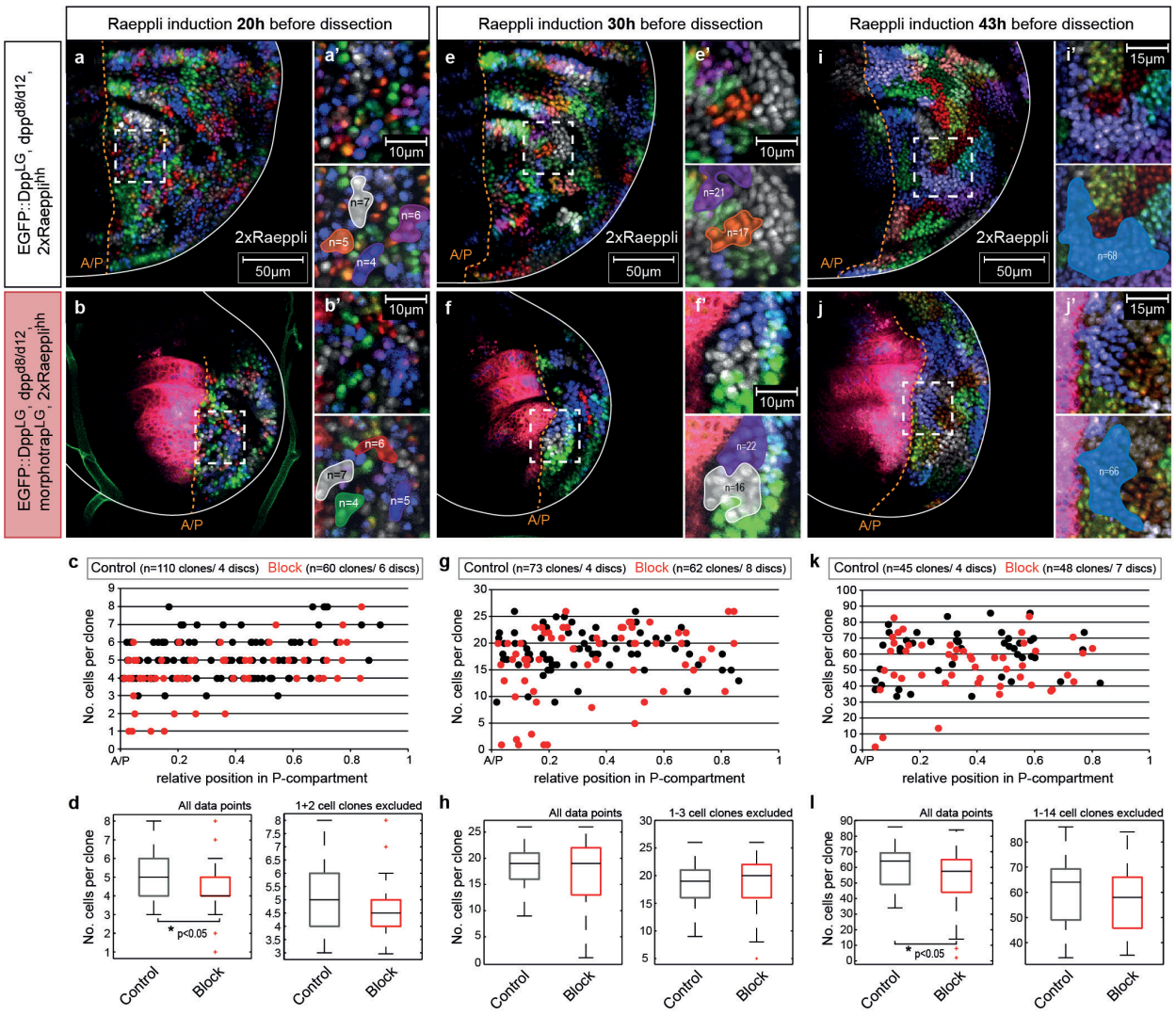

Figure 4 – Block of Dpp spreading does not affect clonal proliferation rates

Estimation of clonal proliferation rates in the posterior compartment using the whole-tissue labelling tool Raeppli. Larvae were staged and dissected at 96-100h AEL. Raeppli was induced at different time points during development: **a-d**, 20h before dissection (78-82h AEL); **e-h**, 30h before dissection (68-72h AEL) and **i-l**, 43h before dissection (55-59h AEL). **c, g, k**, Cell numbers per clone were counted and plotted against the relative position in the posterior compartment (0 corresponding to the A/P boundary and 1 to the posterior edge of the disc). Low numbers of small clones in proximity to the A/P boundary are found in discs with blocked Dpp spreading (red dots), while these small clones are not present in control discs (black dots, also see Extended Data Fig.6). **d, h, I**, Boxplots showing the number of cells per clone. When

the small clones are excluded (right boxplots) no significant differences are detected in clonal proliferation between control discs and discs with blocked Dpp spreading.

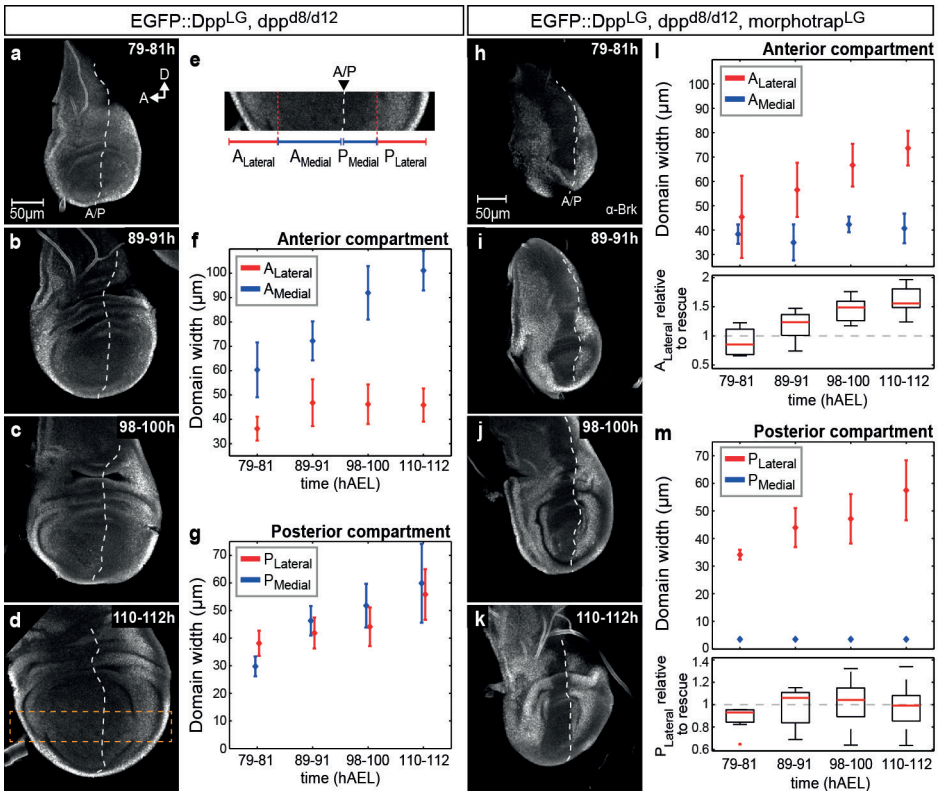

Figure 5 - The development of the medial but not the lateral wing disc requires Dpp spreading

Data set from 79-112h AEL stained for Brk. **a-d**, Representative rescued wing discs of four time points investigated. **e**, Magnification of area marked in (**d**), visualizing the location of medial (high Dpp signalling) and lateral (low Dpp signalling) domain (also see methods for details). **f-g**, Temporal development of domain width in the anterior (**f**) and posterior (**g**) compartment in rescued discs. **h-k**, Representative *dpp*$^{d8/d12}$ mutant wing discs co-expressing EGFP::Dpp and morphotrap. **l-m**, Temporal development of domain width in co-expression wing discs, and relative size change of the lateral domain compared to control discs in the anterior (l) and the posterior compartment (m). The medial region does not increase in width when Dpp spreading is blocked, however the posterior domain ($P_{Lateral}$) increases. (rescue $n = 34$, co-expression $n = 37$, error bars in **f-g** and **l-m** show standard deviation)

Extended Data

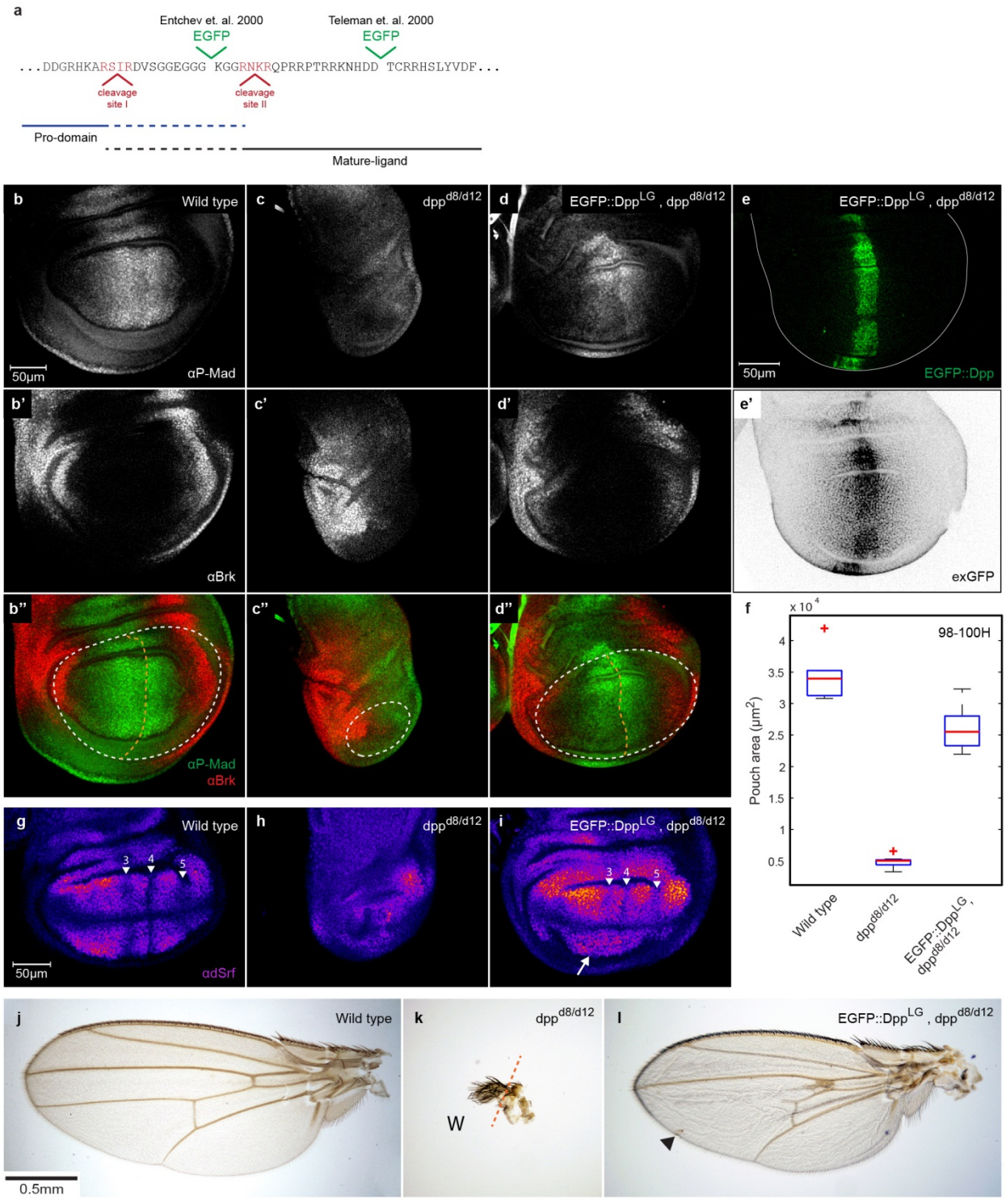

Extended Data Figure 1 – EGFP::Dpp can compensate for endogenous Dpp during wing disc development

a, Part of the protein sequence of the Dpp protein. The two different EGFP insertion sites[9,10], and the two furin cleavage sites[40] located in this region are marked. Furin cleavage of the inactive pro-form yields the active C-terminal mature ligand. However, potential processing at cleavage site II may result in uncoupling of the EGFP from the mature ligand in the Entchev *et.al*[10]. construct. We therefore inserted the EGFP C-terminal to the second furin cleavage site as was done in Teleman *et. al.*[9] **b-d**, Immunostainings for P-Mad and Brk in wild type (**b**), $dpp^{d8/d12}$ mutant (**c**) and $dpp^{d8/d12}$ mutant wing discs rescued with EGFP::Dpp (**d**). In the $dpp^{d8/d12}$ mutant wing discs expressing EGFP::Dpp the P-Mad and Brk profiles are rescued to a control like pattern (**d''**). The pouch outline and the A/P boundary (assessed by Wg/Ptc pattern, not shown) are marked by dotted lines. **e,** The EGFP::Dpp gradient visualized by EGFP fluorescence or by an immunostaining for the extracellular fraction of EGFP (**e'**). **f**, Quantification of wing pouch area of 98-100H old wing discs (wild type $n = 6$, $dpp^{d8/d12}$ mutant $n = 10$, rescue $n = 10$; red cross are outliers). EGFP::Dpp expression in $dpp^{d8/d12}$ mutants rescues pouch area close to wt size. **g-i**, Wing discs of 98-100H old larvae stained for the inter-vein marker dSRF. The vein pattern is largely restored in mutant discs rescued by EGFP::Dpp expression (vein numbers are marked by arrows in (**g, i**)). **j-l**, Adult wings of a wild type fly (**j**), a $dpp^{d8/d12}$ mutant expressing EGFP::Dpp (**k**) and a $dpp^{d8/d12}$ mutant (**l**) (W=wing). Rescued wings have a slightly elongated shape but their sizes are comparable to that of control wings. However they show some additional vein tissue at the anterior cross-vein and wing vein 4 is absent in the distal part of the wing (marked by arrowhead). We speculate that this is due to lower EGFP::Dpp expression in the ventral compartment, which also manifests itself in lower ventral P-Mad levels (see **d**) and less well defined ventral vein patterns in the dSRF staining (**i**, arrow). Apart from these drawbacks, LexA driven EGFP::Dpp can compensate for endogenous Dpp during wing disc development.

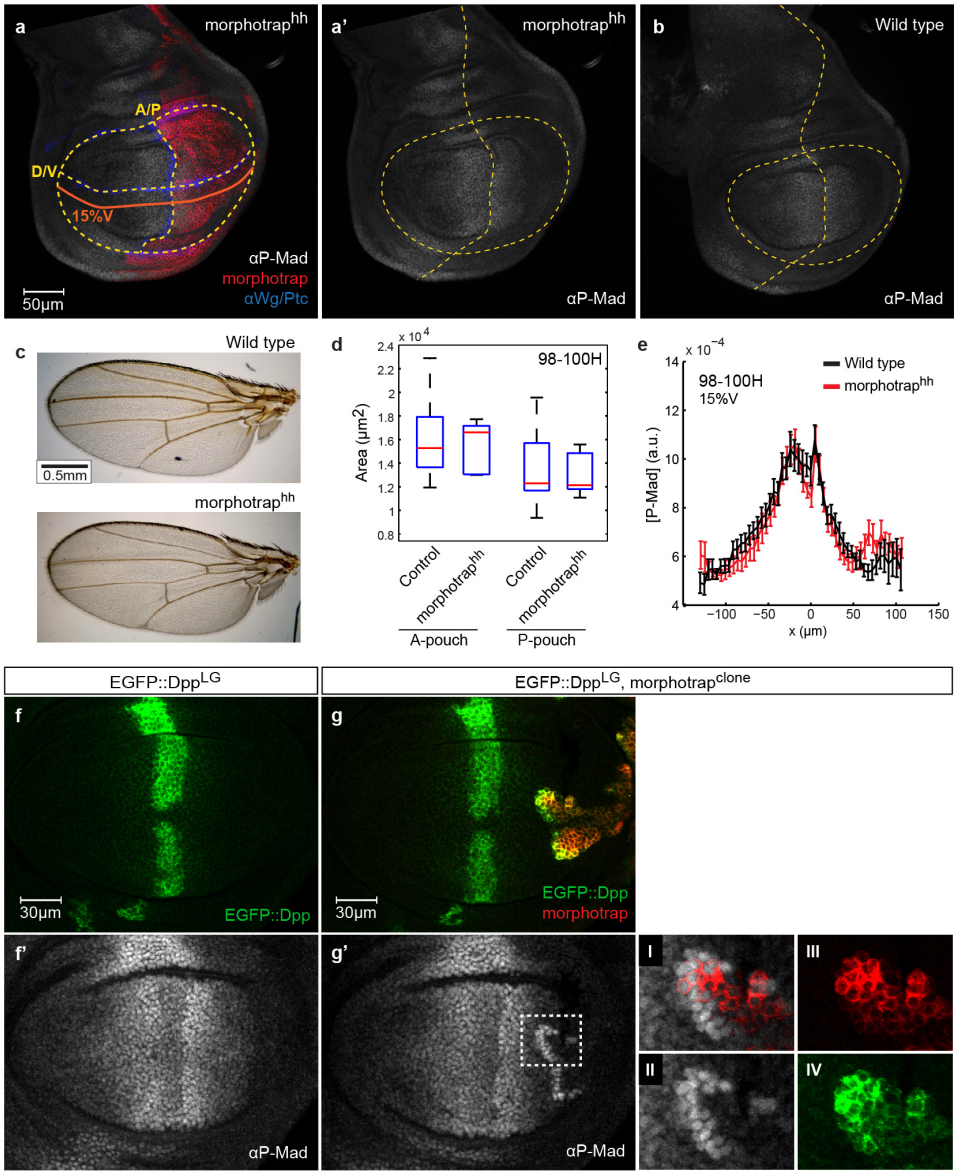

Extended Data Figure 2 – Morphotrap expression does not affect growth or patterning of the wing disc

a, Wing disc expressing morphotrap in the P-compartment controlled by *hh-Gal4* (morphotrap^{hh}). The Wg/Ptc pattern is used as a coordinate system to access pouch size (A-pouch – left two quadrants, P-pouch – right two quadrants). Gradient profiles are measured parallel to the dorso/ventral (D/V) boundary (e.g. 15% ventral offset). **b**, Wild type (wt) wing disc stained for P-Mad. **c**, Wings of male wt and morphotrap^{hh} flies. **d**, morphotrap^{hh} wing discs show no significant change in A- or P-pouch size

compared (*t*-test two-sided, unequal variance: A-comp. $t = 0.85$, P-comp. $t = 0.93$). **e**, Posterior expression of morphotrap does not cause obvious changes to the P-Mad profile. **f**, P-Mad pattern of a wild type wing disc expressing EGFP::Dpp in the endogenous Dpp source. **h**, Lateral morphotrap clones show elevated P-Mad signal at the clone boundary facing the Dpp source due to EGFP::Dpp accumulation. (**d** and **e**: control $n = 11$, morphotrap^{hh} $n = 9$, error bars in (**e**) are standard deviation)

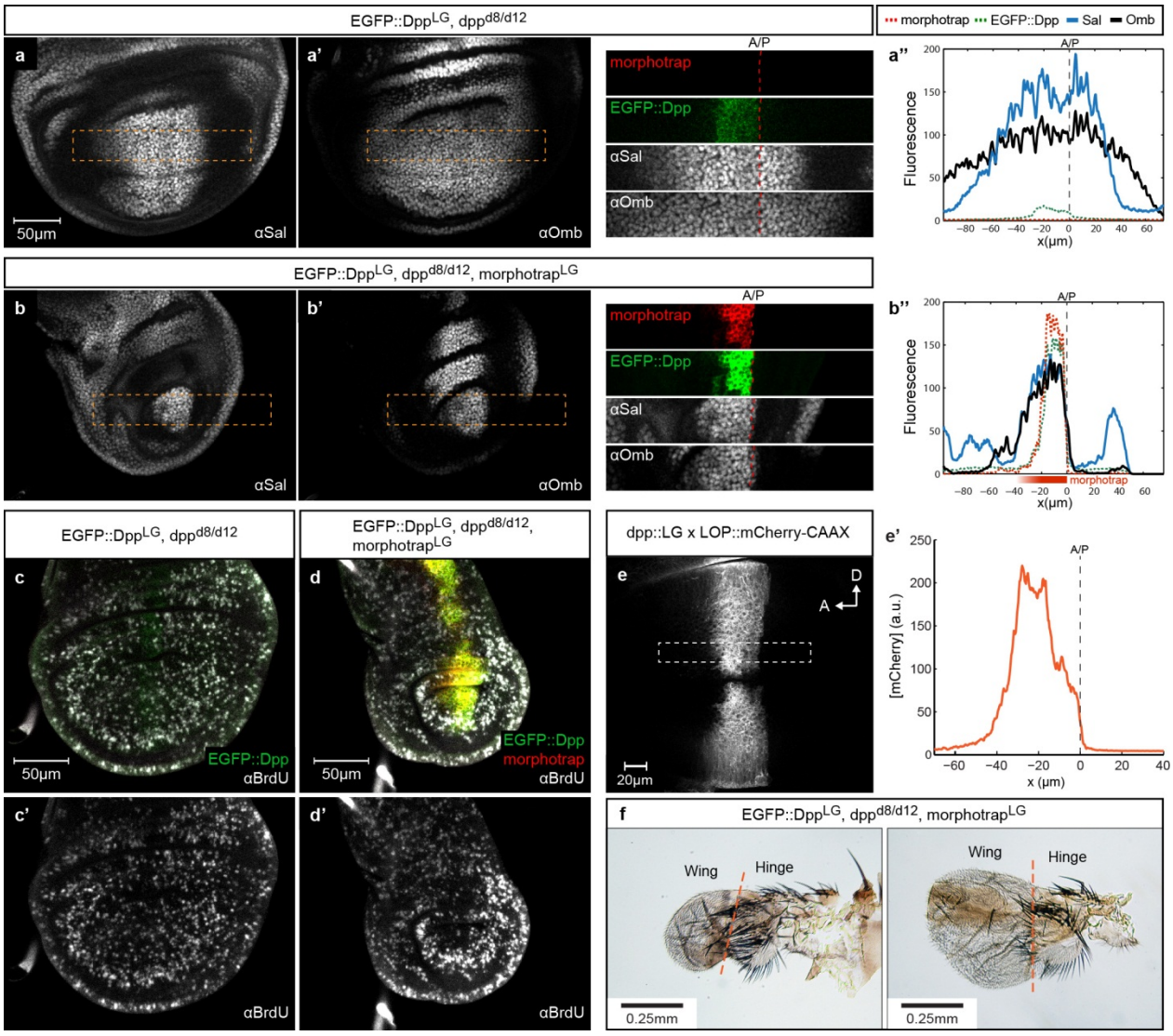

Extended Data Figure 3 - Patterning of Dpp targets directly depends on the Dpp gradient

a, Discs of *dpp*$^{d8/d12}$ mutants rescued with EGFP::Dpp stained for Dpp targets Sal and Omb. Omb shows a wider distribution than Sal. **b**, *dpp*$^{d8/d12}$ mutant wing discs co-expressing EGFP::Dpp and morphotrap. The regions marked by a dotted rectangle are enlarged to the right of the respective image. Red dotted line marks the A/P compartment boundary. In the absence of a Dpp gradient, target domains collapse onto a single cell row in the P-compartment. In the anterior compartment domain borders are less sharp. We hypothesise that this is due to morphotrap bound EGFP::Dpp that is dragged into the A-compartment by dividing cells (also see **e**). Intensity profiles of the enlarged regions are plotted to the right. **c**, Wing disc of a dpp$^{d8/d12}$ mutant rescued with EGFP::Dpp stained for the proliferation marked BrdU. Uniform BrdU

signal is obtained along the entire disc tissue. **d**, Rescued wing disc with blocked Dpp spreading stained for BrdU. Also in the absence of Dpp spreading the uniform BrdU signal is not lost. **e**, Expression of mCherry-CAAX under the control of the *dpp::LexA* driver line used for the rescue. mCherry-CAAX localizes to the membrane and has a long half-life. **c'**, Zoom of the wing pouch region. **c''**, Intensity plot of the region marked in (**c'**). No posterior expression is observed, however the observed protein profile is graded into the anterior compartment. Analogous to morphotrap bound EGFP::Dpp, the stable mCherry-CAAX forms a concentration gradient into the anterior compartment due to dividing cells that are pushed into the A-compartment. f, Wings of rescued flies with blocked Dpp spreading. The hinge region, arising from the lateral wing disc region, is present and well patterned. In contrast, the wing field, arising from the medial wing disc region, is strongly reduced in size and patterning is lost.

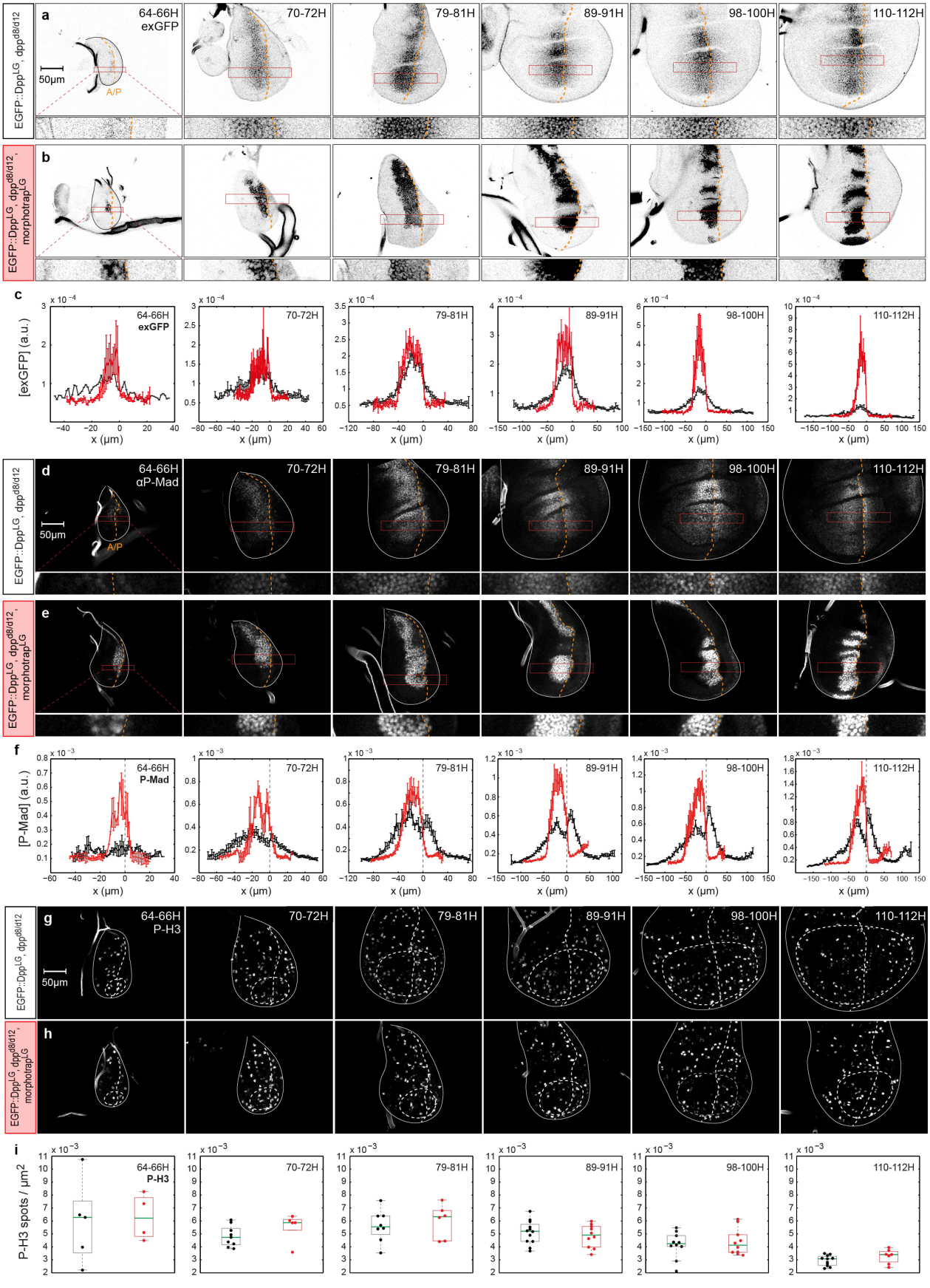
a
64-66H
exGFP
70-72H
79-81H
89-91H
98-100H
110-112H
50µm
A/P
EGFP::Dpp^LG, dpp^d8/d12
b
EGFP::Dpp^LG, dpp^d8/d12, morphotrap^LG
c
[exGFP] (a.u.)
64-66H
exGFP
x (µm)
d
64-66H
αP-Mad
e
f
[P-Mad] (a.u.)
64-66H
P-Mad
g
64-66H
P-H3
h
i
P-H3 spots / µm2
64-66H
P-H3

1

Extended Data Figure 4 – Time course of EGFP::Dpp spreading, signalling and the mitotic index

Time course of extracellular EGFP::Dpp (exGFP), Dpp signalling (P-Mad) and Phospho-Histone3 (P-H3) from 64-112h AEL of larval development. **a-b** , Representative discs of the six time points examined of control animals (**a**) and animals with blocked Dpp spreading (**b**) stained for exGFP. The region marked by a red rectangle is enlarged below each image. EGFP::Dpp spreading is tightly blocked by morphotrap in all time points. **c**, Average exGFP profiles for all time points (control in black /block in red: n=43/29). **d-e**, Discs of control animals (**d**) and animals with blocked Dpp spreading (**e**) stained for P-Mad. When Dpp spreading is blocked, also the P-Mad gradient collapses onto the source region for all time points. **f**, Average P-Mad profiles (control/block: n=50/35). **g-h**, Discs stained for P-H3 of control discs (**g**) and discs with blocked Dpp spreading (**h**). **i**, Quantification of the mitotic index (P-H3 spot density). No significant differences were observed between control discs (black, n=55) and discs with blocked Dpp spreading (red, n=43) at any time point.

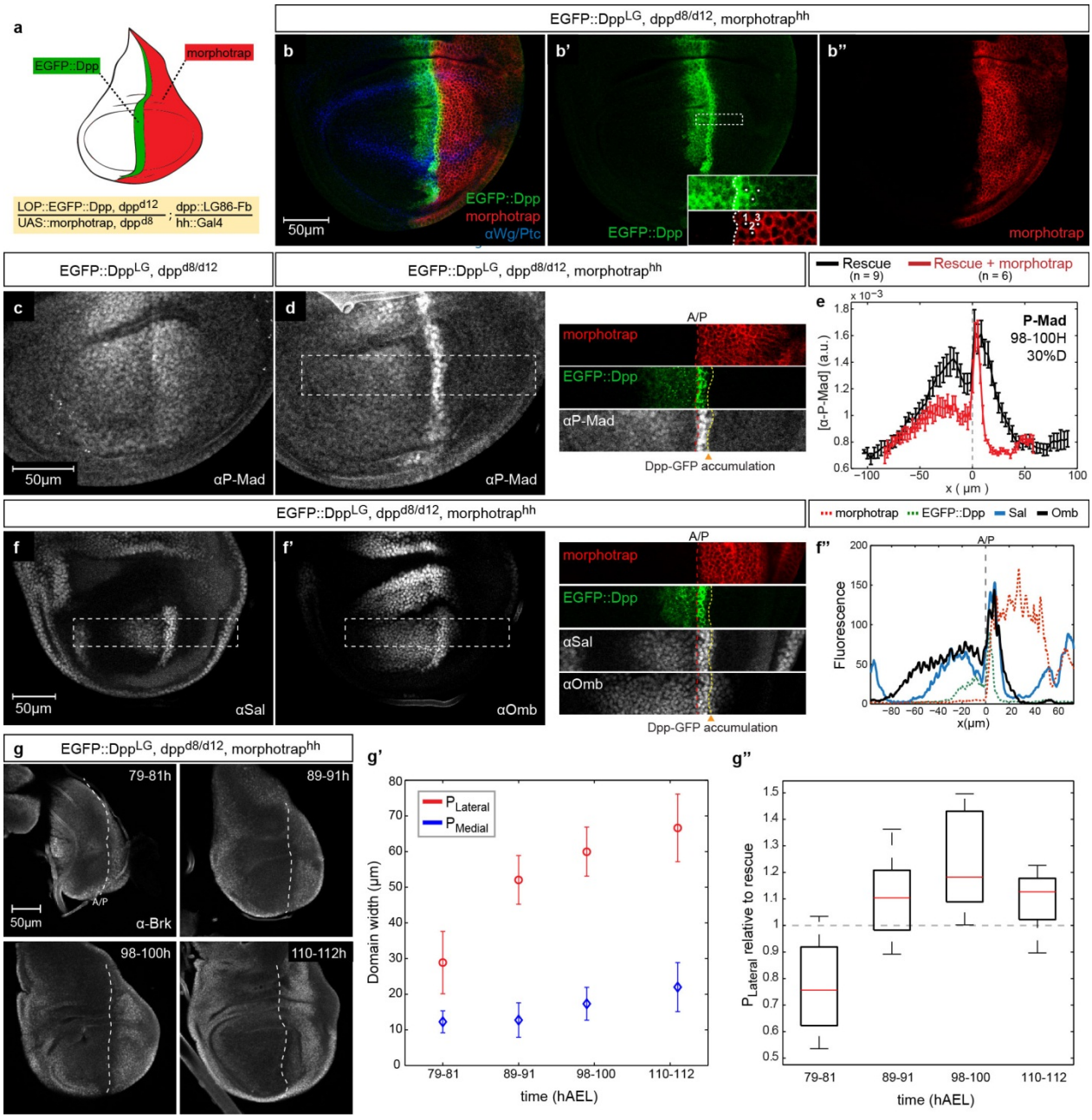

Extended Data Figure 5 – Shortening of the Dpp gradient by posterior morphotrap expression

a, Scheme of morphotrap expression in the posterior compartment in *dpp*$^{d8/d12}$ mutant wing discs rescued with EGFP::Dpp. **b**, Posterior morphotrap expression in the rescue background results in strong EGFP signal in the first 3 cell rows of the P-compartment due to EGFP::Dpp accumulation; after 3 cell rows the EGFP fluorescence signal drops. **c**, P-Mad staining in a *dpp*$^{d8/d12}$ mutant wing discs rescued with EGFP::Dpp. **d**, P-Mad staining in a *dpp*$^{d8/d12}$ mutant wing discs rescued by EGFP::Dpp and expressing

morphotrap in the P-compartment. Note that the EGFP::Dpp accumulation (marked by a yellow line) directly overlaps with the observed P-Mad signal. **e**, The average P-Mad profiles show that the P-Mad gradient range directly depends on the formation of the Dpp gradient (error bars are standard deviation). **f**, $dpp^{d8/d12}$ mutant wing discs rescued with EGFP::Dpp expressing morphotrap in the P-compartment stained for Sal and Omb (for control discs see Extended Data Figure 3a). The A/P boundary is marked by a dotted red line and the range of the EGFP::Dpp accumulation is marked by a dotted yellow line. In this condition the domain widths of both targets are strongly reduced. The Sal domain directly collapses onto the EGFP::Dpp accumulation domain. However Omb, which can be activated at lower Dpp signalling levels, shows a slightly wider distribution. We hypothesis that this is again due to morphotrap stabilized EGFP::Dpp being dragged into the P-compartment (as discussed in Extended Data Figure 4). Intensity profiles of the enlarged regions are plotted to the right (**f''**). **g**, Representative $dpp^{d8/d12}$ mutant wing discs rescued with EGFP::Dpp expressing morphotrap in the P-compartment stained for Brk at the indicated time points (79-112h AEL). In this condition the medial region shows strongly reduced growth (compare to Figure 4**g**). However the growth dynamics of the lateral domain are similar to the lateral growth observed in control wing discs (**g''**).

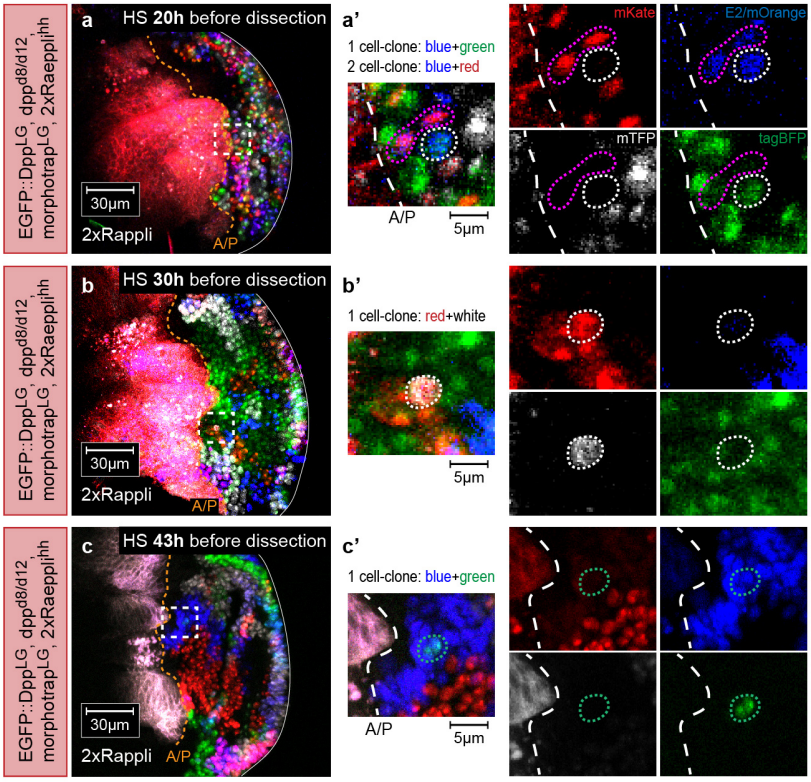

Extended Data Figure 6 – Small clones in discs with blocked Dpp spreading

Wing discs with blocked Dpp spreading and posterior Raeppli expression carrying small clones in proximity of the A/P boundary. Raeppli was induced at different time points during larval development: 20h (**a**), 30h (**b**) and 43h (**c**) before dissection. The regions marked by a white rectangle in the left column (**a,b,c**) are magnified to the right (**a',b'c'**).

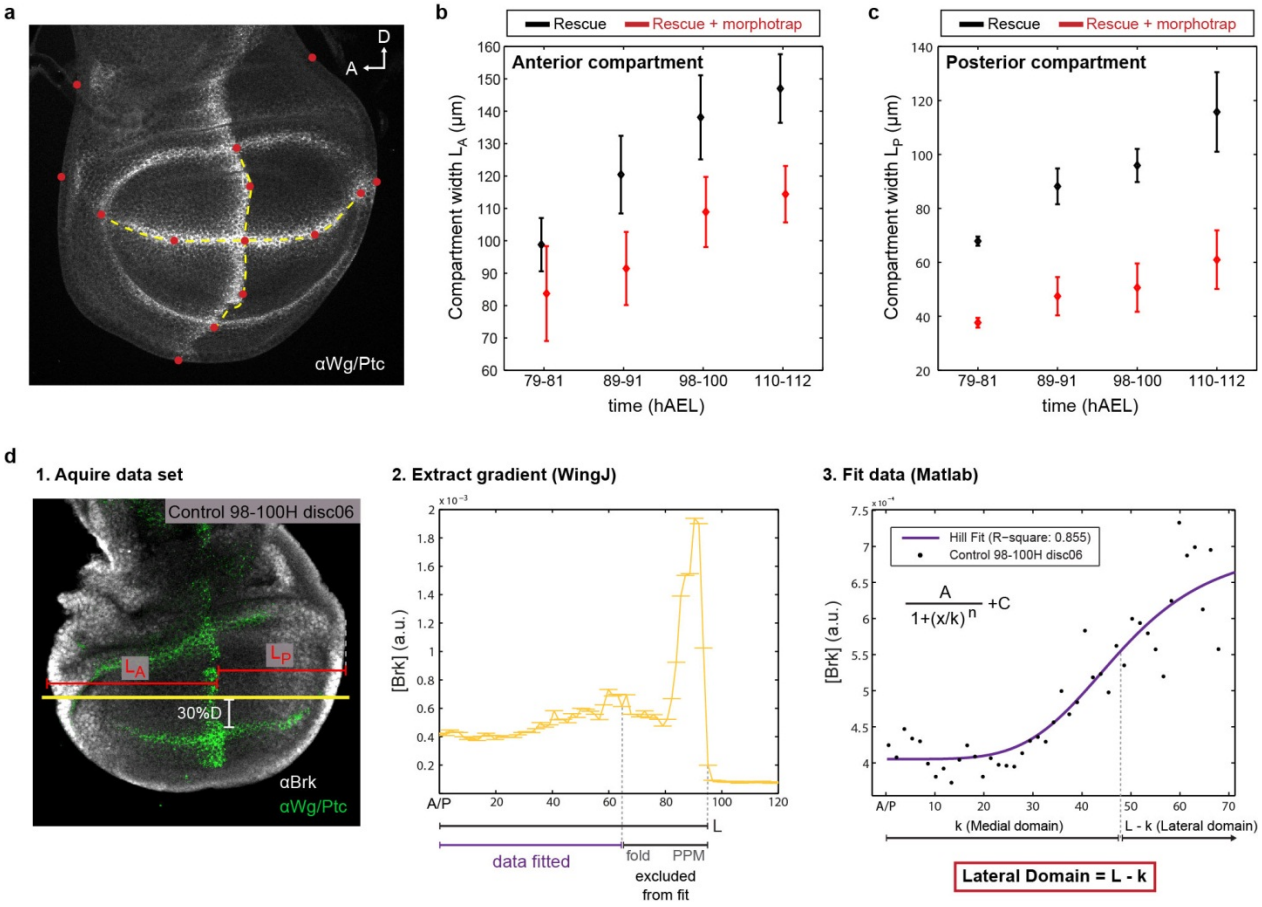

Extended Data Figure 7 - Temporal development and fitting procedure of Brk dataset

a, Red dots mark the 15 landmarks used for affine transformation while generation of mitotic density maps (see Methods). **b-c**, Width of the anterior and posterior compartment respectively in *dpp*$^{d8/d12}$ mutant wing discs rescued with EGFP::Dpp (black) and *dpp*$^{d8/d12}$ mutant wing discs co-expressing EGFP::Dpp and morphotrap (red) (n = 77, error bars are standard deviation). **d**, Computation of Brk data-set shown for the P-compartment: (1) The compartment width L_A or L_P was defined as the distance from the A/P boundary to the anterior or posterior edge of the wing tissue respectively. Brk profiles were measured along a straight line with 30%D off-set. (2) Profiles were extracted using WingJ software. (3) The single gradients were fitted to the shown Hill-function. The fitting procedure return the parameter k, which corresponds to the position of half-maximum Brk levels and hence to the width of the medial domain. Therefore the lateral domain equals L – k.

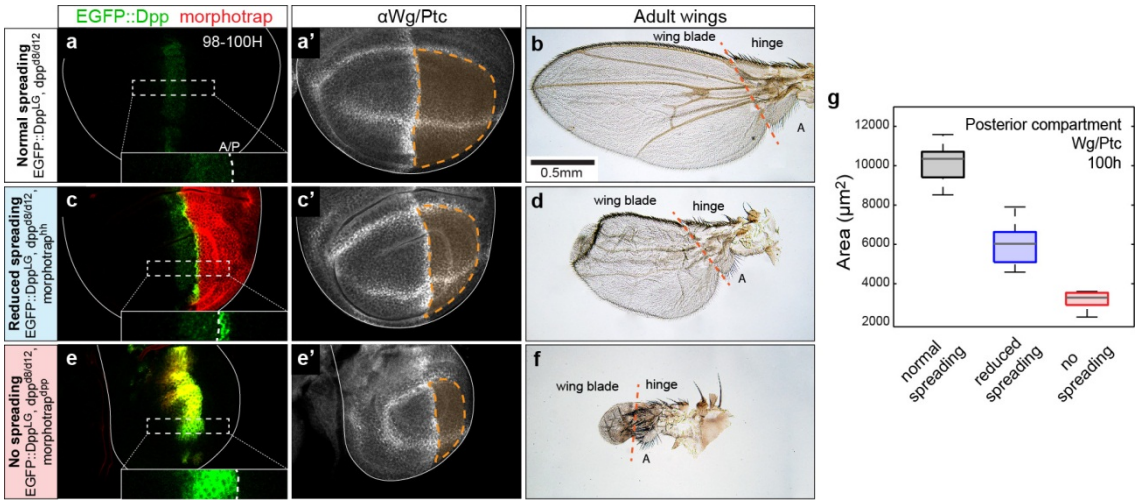

Extended Data Figure 8 - Impact of Dpp spreading on wing pouch and adult wing size

a, Dpp mutant wing disc rescued with EGFP::Dpp stained for Wg, marking the outlines of the wing pouch and Ptc, marking the A/P boundary. In this background EGFP::Dpp spreading is not hindered and a normal gradient forms. The size of the posterior (P) wing pouch is estimated by the area enclosed by the Wg ring and the A/P boundary (marked by Ptc) and plotted in (**g**). **b**, Adult wing of a rescued fly. The border between the hinge region and the wing blade is marked by a dotted orange line; the alula is labelled with an A. **c**, Rescued wing disc expressing morphotrap in the posterior compartment, reducing Dpp dispersal range in the P-compartment. In this condition pouch size is significantly decreased (see **g**). **d**, Wing of a rescued fly expressing morphotrap in the posterior compartment. Wing blade area is strongly decreased and patterning in the posterior part of the wing is lost. **e**, Rescued wing disc expressing morphotrap in the Dpp stripe, completely blocking Dpp spreading, hence gradient formation. Full block of Dpp spreading results in a further decrease of the Wg/Ptc-encircled pouch area. **f**, Wing of a rescued fly co-expressing EGFP::Dpp and morphotrap. Full block of Dpp spreading results in a strong reduction of wing blade area. Only a small amount of unpatterned wing tissue is left, while the hinge region seems to be patterned ok (alula is present). **g**, Plot of the P-pouch area, as accessed by the Wg/Ptc staining shown in (**a'**,**c'**,**e'**) when Dpp spreads normally (black), Dpp spreading is reduced (blue) or when Dpp spreading is fully blocked (red). With decreasing Dpp dispersal range also the P-pouch area decreases. (n = 22)

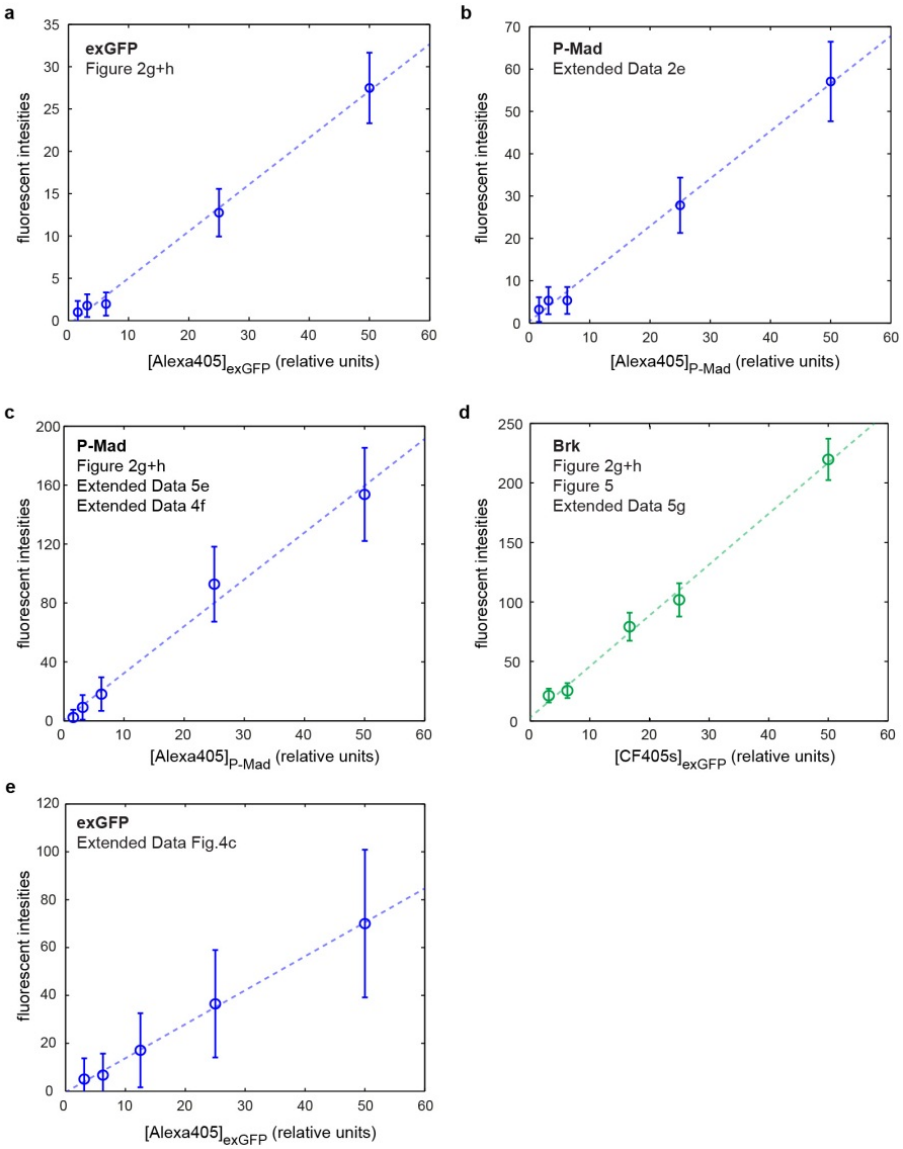

1

2 **Extended Data Figure 9 – Linear range imaging conditions**

3 Linear range imaging for the quantitative data-sets acquired (corresponding figure is labelled at top left in
4 each plot). Dilutions of the secondary antibodies used (anti-rb-Alexa 405 (blue) and anti-gp-CF405S
5 (green)) in Vectashield mounting medium yield fluorescent intensities proportional to their concentrations
6 under the established imaging conditions. Mean intensities we extracted using the Histogram function in
7 ImageJ on the whole imaging field of a mean projection. The background fluorescence was measured by
8 imaging a slide only containing Vectashield and subtracted from the mean values. Dotted lines indicate
9 linear fits.